ESC-TR-95-058

Technical Report
1029

Anomalous Magnetoresistance in the Lanthanide Manganites and Its Relation to High-T_c Superconductivity

G.F. Dionne

20 May 1996

Lincoln Laboratory
MASSACHUSETTS INSTITUTE OF TECHNOLOGY
LEXINGTON, MASSACHUSETTS

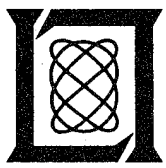

Prepared for the Department of the Air Force under Contract F19628-95-C-0002.

This report is based on studies performed at Lincoln Laboratory, a center for research operated by Massachusetts Institute of Technology. The work was sponsored by the Department of the Air Force under Contract F19628-95-C-0002.

The ESC Public Affairs Office has reviewed this report, and it is releasable to the National Technical Information Service, where it will be available to the general public, including foreign nationals.

This technical report has been reviewed and is approved for publication.

FOR THE COMMANDER

Gary Tutungian
Administrative Contracting Officer
Contracted Support Management

MASSACHUSETTS INSTITUTE OF TECHNOLOGY
LINCOLN LABORATORY

ANOMALOUS MAGNETORESISTANCE IN THE LANTHANIDE MANGANITES AND ITS RELATION TO HIGH-T_c SUPERCONDUCTIVITY

G.F. DIONNE
Group 63

TECHNICAL REPORT 1029

20 MAY 1996

LEXINGTON MASSACHUSETTS

ABSTRACT

A theory of electron transport is formulated from the polaronic and magnetic exchange character of mixed-valence transition metal oxides. Where magnetic ordering is established at low temperatures, the conduction is mainly by polarons. Above the Curie temperature T_C, electron hopping by thermal activation becomes dominant. The conventional relations for mobility-activated semiconduction and the molecular field theory of ferromagnetism are adapted for interpretation of electrical resistivity ρ data of the lanthanide (rare-earth—*RE*) manganites $(RE^{3+}_{1-x}A^{2+}_{x})MnO_3$ as functions of temperature and external magnetic field. Computed results are consistent with the original resistivity data and agree quantitatively with the more recently observed magnetoresistance in film versions of this oxide system. The anomalies in electrical behavior are related to the superexchange couplings derived from σ and π bonding of the various $3d$ orbital states among $Mn^{2+}(3d^5)$, $Mn^{3+}(3d^4)$, and $Mn^{4+}(3d^3)$ ions in 180° metal-oxygen-metal configurations. The resistivity maximum occurs at the susceptibility peak slightly above T_C, and its magnitude is determined principally by the factor $[(1-x)/x]\ (kT_C)\ \exp(E_{hop}/kT_C)$, where the activation energy E_{hop} is the sum of a polaron trap energy $E_{hop}{}^0$ (~ 5 meV) and a spin polarization-dependent component $E_{hop}{}^{ex}[1-B_S(T,H)]$, and B_S is the Brillouin function. For $T \geq T_C$, ferromagnetic spin alignment becomes disordered and E_{hop} increases to a value ~ 0.1 eV equal to the decrease in stabilization energy of the transfer electrons caused by the transition from spin alignment to disorder, i.e., $B_S = 0$. If E_{hop} is independent of temperature above T_C, the maximum sensitivity $d\rho/dH$, which occurs at $T = T_C$, may be exclusively a function of T_C through the function $(1/kT_C)\ \exp(E_{hop}/kT_C)$. The relative sensitivity $(1/\rho)d\rho/dH$, however, is not dependent on the exponential factor but is proportional to $1/T_C{}^2$. As expected, the magnetoresistance sensitivities favor uniformity of T_C, and consequently a high degree of chemical homogeneity in the material.

A similarity exists between the metallic ρ of the multivalent manganites at low temperatures and that of the superconducting cuprates. In both cases the basic theory of the hopping electron semiconductor applies with almost identical values of lattice parameter and Debye frequency. However, the magnetic exchange contribution to E_{hop} in the manganite system differs from that of the cuprates. In the former case, the sharp decrease in the ferromagnetic exchange field at T_C enhances the magnetic field influence on ρ. It also correspondingly raises E_{hop} to reverse the resistivity from metallic to insulating. In the latter case, the absence of long range antiferromagnetic order due to the presence of zero-spin Cu^{3+} ions removes the exchange contribution to E_{hop}. In both the manganites and cuprates, it is concluded that metallic resistivity occurs because of the absence of an exchange trap.

ACKNOWLEDGMENTS

The author is indebted to Dr. Y-Q. Li of NZ Applied Technologies for providing prepublication access to his measurement data, to Dr. R.C. O'Handley of the MIT Department of Materials Science and Engineering for guidance in the progress of experimental work in this field, to Prof. J.B. Goodenough of the Center for Materials Science & Engineering at the University of Texas at Austin for some enlightening comments on the subtleties of magnetic exchange in transition-metal oxides, and to Dr. K.B. Hathaway of the Office of Naval Research for recommending the magnetoresistance effect in the manganites as a subject for investigation.

TABLE OF CONTENTS

LIST OF ILLUSTRATIONS

LIST OF ILLUSTRATIONS (Continued)

LIST OF TABLES

1. INTRODUCTION

Recent observations of anomalous reductions in electrical resistivity of lanthanide manganese perovskites under the application of strong external magnetic fields [1] have prompted a reexamination of the seminal work on the electronic properties of mixed-valence manganites. Original magnetic studies on $(RE^{3+}A^{2+})MnO_3$, where RE^{3+} represents any trivalent member of the lanthanide series and A^{2+} would be ions of Ca, Sr, Ba, or Pb, were reported by Jonker and Van Santen in 1950 [2]. A follow-up note [3] reported an enlightening correlation between the electrical resistivity and the magnetic properties as functions of Sr^{2+} concentration and temperature. At the time of these early observations from powder specimens, the source of the unusual magnetic properties that featured a curious mix of ferro- and antiferromagnetism provided a challenge for the theorists who were developing rules for superexchange in transition-metal oxides [4–6].

Van Santen and Jonker [3] reported the characteristic peak in resistivity at the Curie temperature T_C as a function of temperature, similar to that observed recently in film versions of this compound, as shown in Figure 1. For reasons related to the unavailability of textured or single-crystal film specimens, the magnitude of the effect was substantially reduced from that reported in Jin et al. [1]. Furthermore, magnetoresistance was not investigated in this early work, and the anomalously large effects could not have been detectable with the kilo-oersted magnetic field strengths available at that time.

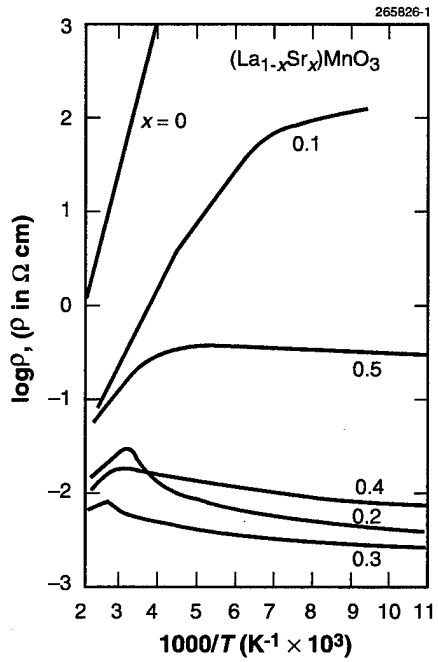

Figure 1. Original observation of the metal-semiconductor transition in $(La_{1-x}Sr_x)MnO_3$ by Van Santen and Jonker [3].

This report reviews the electrical conduction mechanisms of polarons and electron hopping in partially covalent and ionic compounds; the magnetic data of the bulk material are analyzed in terms of the conventional wisdom of magnetic exchange. An empirical model is then constructed to fit the measured variation of Curie temperature with composition in the generic manganite family. The combined theories of electrical conduction and spontaneous magnetism are then used to fashion a phenomenological theory of magnetoresistance suitable for estimating the performance of potentially magnetoresistive compounds. Finally, to place the low-temperature electrical behavior in a more expanded context, the charge transfer mechanisms of the $Mn^{3+} \leftrightarrow Mn^{4+} + e^-$ combination are compared with those of $Cu^{2+} \leftrightarrow Cu^{3+} + e^-$ and $Cu^{1+} \leftrightarrow Cu^{2+} + e^-$ conduction of the high-T_c superconducting cuprates.

2. CHARGE TRANSPORT AND STABILIZATION ENERGY

Metal oxides with d^n series transition ions are basically ionic compounds, but feature a covalent component that arises from unfilled d shells of the cations that couple to each other through the medium of the oxygen O^{2-} anion lattice. When the transition metal ions are of mixed valence because of vacancies or chemical substitutions, charge carriers may transfer among the cations of similar elements through the oxygen anions, e.g., $Mn^{3+}(d^4) \leftrightarrow Mn^{4+}(d^3) + e^-$, as a normal part of the covalent bonding. This electron sharing by actual charge transfer, therefore, can lower the free energy of the bonding system by broadening the electronic energy states into bands. The mobility of the carriers is determined principally by the overlap integrals between the cation and anion orbital states which give rise to electron exchange that is influenced by temperature and the state of magnetic order. The exchange mechanism allows charge transfer to occur by tunneling without the expense of an excitation energy to establish an intermediate molecular state of higher ionization potential.

The analysis of charge movement in these materials is carried out in two steps: first, the transfer of electrons among sites of equivalent energy, depicted as locations around the rings in Figure 2, and second, the transport of charges to higher energy sites in the lattice, depicted by the transitions to the outer ring. In the first case, the gain in binding energy is of kinetic origin, being derived directly from the actual transfer of charge, and therefore favors a large covalent exchange energy integral to stabilize the transfer ground state; in the second the stabilization results from a standard Coulomb potential well or trap, but favors a small exchange integral to lengthen the carrier lifetime in the trap. Because the exchange energy plays opposite roles in determining the carrier mobility activation in these two situations, they are not readily combined in the same perturbation calculation. The stabilization energy associated with charge transfer is critically related to the states of spin polarization of the transfer ions and is a central factor in the anomalous magnetoresistance effect. Charge transport to higher energy sites, however, can be examined from the standpoint of polaron theory independent of magnetic exchange issues, and will be dealt with first.

2.1 POLARON ACTIVATION ENERGY

The electrical conductivity by weakly bound electrons from this mixed-valence condition is often referred to as polaronic, which follows from the fact that the carrier combined with the lattice electrostatic and elastic energy trap in which it resides is called a polaron. In his treatise on polarons [7], Holstein defined three stages of conductivity that were determined by the relative magnitudes of two energy parameters: (i) the polaronic charge transfer energy b_p, which establishes the lifetime τ_p of the polaron carrier in its site according to $\tau_p \sim \hbar/b_p$, and thereby presents b_p as the width of the energy band, and (ii) the energy ΔE_p of the electrostatic potential well in which the carrier resides and which is shaped by the charge of the carrier and a neighboring charge of opposite sign that created it, i.e., the other half of an extendible dipole. As outlined in the Appendix, b_p is directly related to the covalent exchange integral b_t between the two transfer cations which acquire their overlap integrals indirectly through the immediate cation-anion overlaps. The stabilization energy $E_{hop}{}^0 = \Delta E_p{}^2/8b_p$ that emerges from the calculation becomes the activation energy required for charge transport to the second cation site of ΔE_p higher energy, e.g., to a site on the outer ring in Figure 2.

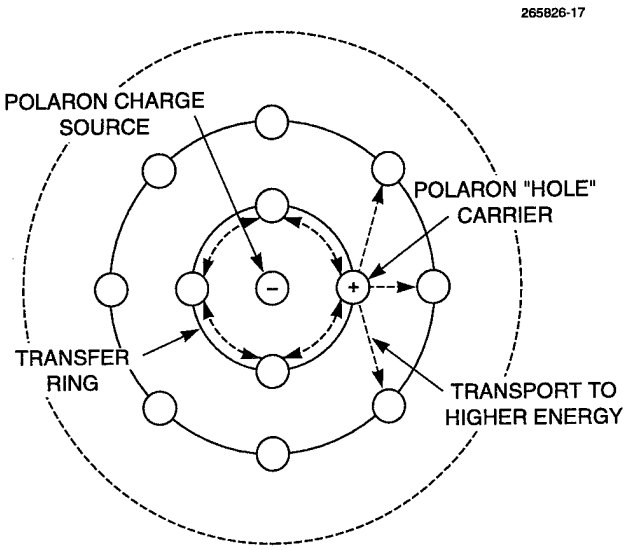

Figure 2. Polaronic activity, including carrier transfers among covalently linked sites that are equivalent with respect to the central fixed ionic charge and transport to sites of higher energy normally farther from the polaron source.

Based on these concepts, Holstein defined the criterion for a large polaron (one in which the carrier extends beyond its immediate environment and allows spontaneous charge transfer) as $b_p >> E_{hop}{}^0$, and that of a small polaron (which is limited to its immediate neighboring sites) as $b_p < E_{hop}{}^0$. In the final stage which sets in at higher temperatures, the metallic conductivity begins to break down and semiconduction by incoherent electron hopping becomes dominant. With increasing temperatures the large polaron condition begins to fail because higher frequency lattice vibrations allow the carriers to stabilize in their traps by permitting elastic adjustments to occur more quickly, thereby lengthening the polaron lifetime of τ_p. This action is represented as a decrease in b_p which begins to set in as the temperature approaches the Debye temperature Θ_D (see footnote 3 in the Appendix).

As a consequence, the decrease in b_p will eventually raise $E_{hop}{}^0$ and reduce the hopping electron population according to a probability approximated by the Boltzmann relation $p_p = \exp(-E_{hop}{}^0/kT)$ in the usual diffusion relation for electron hopping by thermal activation. The conversion of a polaron carrier into a hopping electron, therefore, requires that an increase in thermal energy $E_{hop}{}^0$ be supplied to remove it from its trap. Based on estimates from the simple model in the Appendix, $E_{hop}{}^0 \approx 5$ meV at low temperatures.

In the absence of a magnetic exchange trap that could suppress polaron conduction, the probability p_p represents the statistical partitioning of coherent polaron carriers from incoherent activated carriers. At $T = 0$ all the carriers are polaronic and therefore produce a metallic resistivity. As T increases, thermal activation initially follows an insulating resistivity slope with temperature, but switches to metallic when

kT exceeds E_{hop}^{0}. As a result, the issue of whether the carriers are polaronic or activated is not of great importance in the metallic region of the manganites. For superconductivity in the cuprates, however, the partition of carriers between covalent and hopping electrons is crucial in determining the fraction of carriers that can conduct coherently. In this case the critical temperature T_c is determined by the concentration of coherent polaron carriers and is therefore reduced by the occurrence of incoherent thermal activation.

2.2 EXCHANGE ACTIVATION ENERGY

Before the charge can be transported from its site of minimum energy to one of higher energy, it first must be able to transfer between similar ions through an exchange-assisted ionization process, i.e., around the rings in Figure 2. As explained in the Appendix, the charge transfer produces a stabilization energy $E_{ex} = (b_t^2/2U)(1 + \cos\theta)$, where b_t is the exchange integral between the two cations, U is the energy of the excited state involving the anion that mediates the transfer between cations, and θ is the angle between the direction of a spin and that of the average exchange field in which it resides. To relate E_{ex} to an activation probability, one needs only to recognize that any loss of this binding energy because of spin canting ($\cos\theta < 1$) translates directly into the energy that must be supplied to restore the spin alignment of the transfer ions. Therefore, the exchange activation energy of the magnetic trap may be expressed as $E_{hop}^{ex} = (b_t^2/2U)(1 - \cos\theta)$, which is zero in the $\theta = 0$ ferromagnetic state, but reaches $b_t^2/2U$ in the $\theta = \pi/2$ paramagnetic state above the Curie temperature. Theoretically, the absolute maximum of b_t^2/U occurs in the hypothetical case of $\theta = \pi$, where the system would convert to antiferromagnetism.

This "magnetic trap" energy E_{hop}^{ex} is thus based on the $\Delta S = 0$ selection rule for charge transfer in magnetic oxides. If the stabilization that results from the activationless carrier mobility is lost because of spin misalignment, additional energy is then required to restore the $\Delta S = 0$ condition. Under the preceding conditions, the stabilization is the result of kinetic exchange processes of electron delocalization through covalent interaction with oxygen. E_{hop}^{ex}, therefore, represents this energy discrepancy, which appears as an additional energy barrier that must be surmounted in order to allow the charge transfer to proceed. Similar to that of polaron transport, a transfer probability derived from the exchange interaction may be defined as $p_{ex} = \exp(-E_{hop}^{ex}/kT)$, and after combining transfer and transport activation [see Equation (A-14) in the Appendix], an overall probability of carrier activation becomes $p = p_p p_{ex} = \exp(-E_{hop}/kT)$, where $E_{hop} = E_{hop}^{0} + E_{hop}^{ex}$.

Metallic conductivity occurs with $Mn^{3+}(d^4) \leftrightarrow Mn^{4+}(d^3) + e^-$ ferromagnetic couplings in $(RE^{3+}_{1-x}A^{2+}_{x})[Mn^{3+}_{1-x}Mn^{4+}_{x}]\ O_3$ compounds that feature large magnetoresistance effects at the Curie temperature. For $x < 0.5$, the spin alignment is reinforced because the Mn^{3+}-O^{2-}-Mn^{3+} superexchange is also ferromagnetic through the influence of a vibronic Jahn-Teller (J-T) effect [8]. Another situation where $b_p > E_{hop}$ and metallic behavior is observed occurs where the spin alignment and the $\Delta S = 0$ issues are moot because one of the spins is zero. If the density of $S = 0$ polarons is high enough to frustrate long-range antiferromagnetic order, $E_{hop}^{ex} = 0$. Familiar examples of this situation are the $Cu^{2+} \leftrightarrow Cu^{3+}$ $(S = 0) + e^-$ and $Cu^{1+} \leftrightarrow Cu^{2+} + e^-$ charge transfers of the high-T_C superconducting cuprates. Other compounds where polaronic conductivity occurs at low temperatures without magnetic constraints are the

mixed valence Ti, V, and Bi oxides, where superconducting properties have been reported. In the ferroelectric perovskite $BaTiO_3$, dielectric absorption of microwave energy may be related to the intrinsic polaronic nature of the compound in the presence of imperfect stoichiometry.

TABLE 1

Conduction Mechanism Thresholds

$b > E_{hop}$	Large polarons, covalent transfer, coherence, (collective electrons, metallic ferromagnetism)
$b < E_{hop}$	Small polarons, covalent transfer, coherence, band narrowing by lattice vibrations
$b << E_{hop}$	Narrowbands, semiconducting, incoherence, hopping electrons

3. MAGNETIC PROPERTIES OF $(RE^{3+}A^{2+})MnO_3$

3.1 MAGNETIC EXCHANGE

In the generic $(RE^{3+}A^{2+})MnO_3$ system, all three oxidation states of Mn can occur, offering a variety of 180° superexchange interactions. For the basically cubic octahederal oxygen coordination, crystal-field effects dictate that the t_{2g} orbital states are of lower energy and half-filled to satisfy the Hund's rule spin polarization requirement for each of $Mn^{2+}(d^5)$, $Mn^{3+}(d^4)$, and $Mn^{4+}(d^3)$. For all combinations of exchange pairs, the t_{2g} electrons produce weak antiferromagnetism via covalent π bonding through the O^{2-} anions, e.g., Mn^{4+}-O^{2-}-Mn^{4+}. For the Mn^{2+} and Mn^{3+} ions, the exchange is determined more by the stronger σ-bonding e_g states. A single electron in the e_g states (Mn^{3+} case) can be stabilized by a static J-T orthorhombic distortion that splits energy levels as shown in Figure 3. Where the distortions are cooperative, a tetragonal/orthorhombic phase will appear with axis ratio $c/a > 1$, and the half-filled d_z2 orbital is stabilized relative to the empty $d_x2_{-y}2$ state.

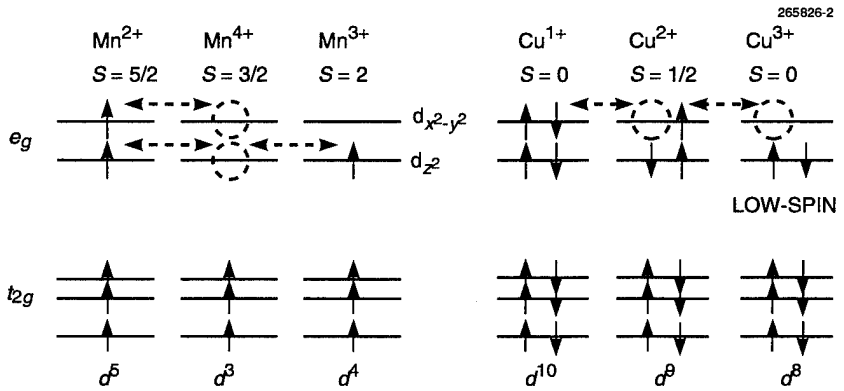

Figure 3. Crystal-field splittings and ground-state orbital occupancies of Mn and Cu ions in octahedral orthorhombically distorted oxygen octahedra. Charge transfers in the e_g states with ferromagnetic spin polarization are indicated.

From the Curie temperature data of Jonker and Van Santen [2] for $(La^{3+}_{1-x}Ca^{2+}_{x})Mn^{3+}_{1-x}Mn^{4+}_{x}O_3$ presented in Figure 4, the variations in exchange field with Mn^{4+} concentration may be analyzed on the basis of changes in the nature of the J-T effect [8]. At $x = 0$, the J-T effect should be mainly static and cooperative, causing an orthorhombic distortion and antiferromagnetic order. With increasing Mn^{4+} concentration, ferromagnetism dominates in the regime up to $x = 0.5$ with a peak near $x = 0.3$. As Mn^{4+} ions are introduced, parallel spin alignments occur through a combination of factors: (i) the Mn^{3+}-O^{2-}-Mn^{4+} couplings produce a kinetic ferromagnetism by charge transfer among half-filled/empty orbital combinations as analyzed in the Appendix and also studied earlier by Zener [9] and de Gennes [10], and (ii) the anticipated antiferromagnetism from the Mn^{3+}-O^{2-}-Mn^{3+} couplings in a static J-T effect

is converted to ferromagnetism by vibronic-induced J-T effects proposed by Goodenough et al. [8] that blurs the identities of the two e_g bands and allows the Mn^{3+} e_g electrons to transfer into empty orbital states. As illustrated in Figure 5, in cases where the Mn^{3+}-O^{2-}-Mn^{3+} couplings dominate and the electronic bandwidth is broad enough for the interactions to be collective, a ligand "breathing" mode may cause the d_z2 and $d_{x^2-y^2}$ states of adjacent Mn cations to oscillate out of phase and form a single band that is only one-quarter filled, giving rise to ferromagnetic order [11]. This quasi-static J-T effect is consistent with the absence of the orthorhombic J-T distortion in the regime of the observed ferromagnetism. The anticipated couplings for the various combinations are summarized in Table 2 [6].

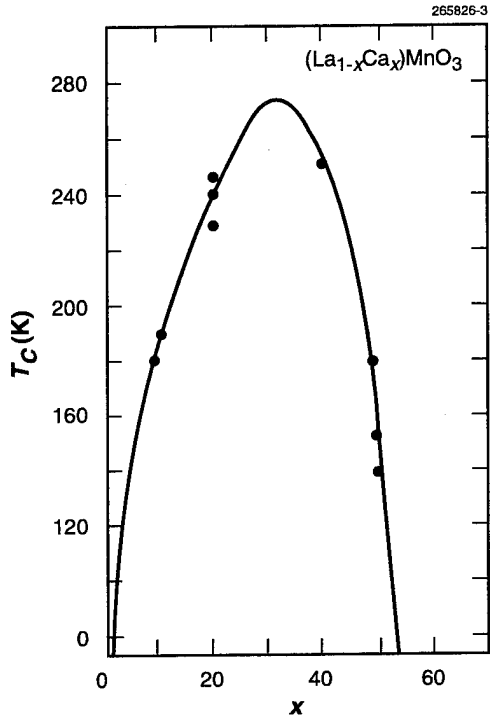

Figure 4. Typical data of T_C versus x for $(La^{3+}_{1-x}Ca^{2+}_{x})Mn^{3+}_{1-x}Mn^{4+}_{x}O_3$. Data are from Jonker and Van Santen [2].

At a point in the regime $x \leq 0.1$, the crystallographic phase changes to rhombohedral (trigonal symmetry with no J-T splitting of the e_g levels) and survives until $x \approx 0.5$. With half the Mn ions in the 4+ state, the quasi-static behavior breaks down, and the remaining Mn^{3+}-O^{2-}-Mn^{3+} couplings revert to antiferromagnetism, combining with weakly antiferromagnetic Mn^{4+}-O^{2-}-Mn^{4+} couplings to produce mainly antiferromagnetism in the range from $0.5 \leq x \leq 1.0$. At higher temperatures, changes in the cation charge distribution could enable the rhombohedral phase to extend beyond $x = 0.5$, exhibiting the peculiar antiferromagnetic/ferromagnetic transition first reported by Jonker and Van Santen [2] for $(La^{3+}_{0.3}Sr^{2+}_{0.7})MnO_3$.

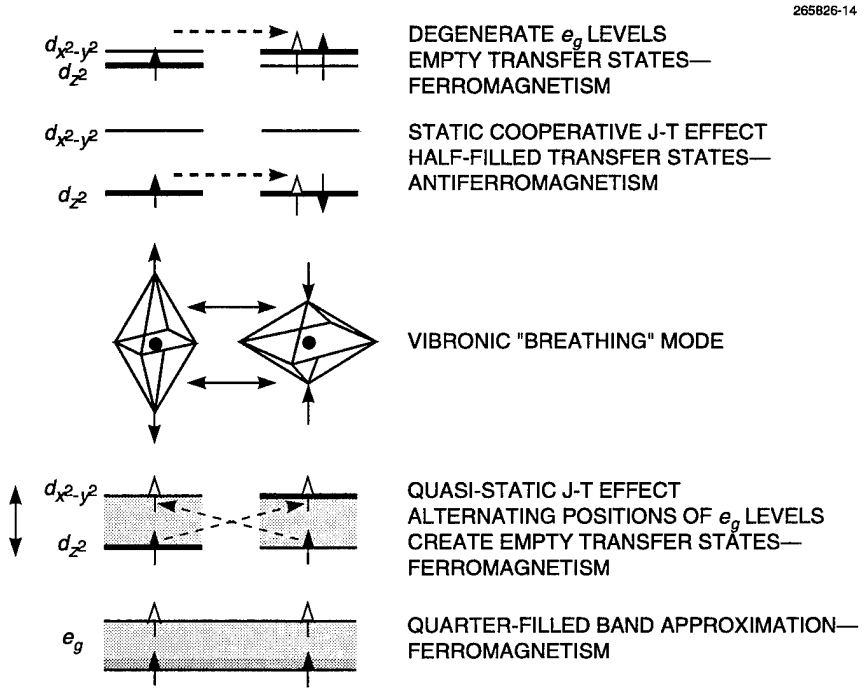

Figure 5. Schematic diagrams of J-T effects, including the quasi-static case in which carrier transfers into empty e_g orbital states that are mixed by vibronic modes may cause ferromagnetism.

3.2 RANDOM DISTRIBUTION APPROXIMATION

If the spatial distribution of Mn^{4+} ions is assumed to be random, the reduction in energy of a spin S_i surrounded by spin S_j due to magnetic ordering as outlined in the Appendix may be approximated from the exchange Hamiltonian $\mathcal{H}_{ex} = -2\sum_j J_{ij}\mathbf{S}_i \cdot \mathbf{S}_j$. To work with positive energies, $E_{ex} = -\mathcal{H}_{ex}$ is defined as the gain in stabilization energy. Because it represents an average of the various interactions between the spins of the Mn^{3+} and Mn^{4+} ions, E_{ex} is expressed as a statistically weighted sum that varies with concentration, according to :

$$\begin{aligned} E_{ex} &= E_{33} + E_{34} + E_{43} + E_{44} \quad , \\ &= 2z\left[p_3{}^2 J_{33} S_3{}^2 + p_3 p_4 J_{34} S_3 S_4 + p_4 p_3 J_{43} S_4 S_3 + p_4{}^2 J_{44} S_4{}^2\right]\cos\theta \quad , \end{aligned} \tag{1}$$

TABLE 2

Magnetic Exchange of d^n Electrons in 180° Bonds[a]

Ion Pair	d_{xy}, d_{xz}, d_{yz}	$d_{x^2-y^2}$ a-b Axes	d_{z^2} c Axis	Net
$d^5 \leftrightarrow d^5$	↑↓π(wk)	↑↓σ(str)	↑↓σ(str)	↑↓ (str)
$d^5 \leftrightarrow d^4$	↑↓π(wk)	↑↓σ(str)	↑↓σ(str)	↑↑ (str) ↑↓ (str)
$d^4 \leftrightarrow d^{4b}$	↑↓π(wk)	↑↓σ(str)	–	↑↓ (str)
$d^5 \leftrightarrow d^{3c}$	↑↓π(wk)	↑↓σ(mod)	↑↓σ(mod)	↑↑ (mod)
$d^4 \leftrightarrow d^{3d}$	↑↓π(wk)	↑↑σ(str)	–	↑↑ (mod)
$d^3 \leftrightarrow d^3$	↑↓π(wk)	–	–	↑↓ (wk)

a. Based on rules developed by J.B. Goodenough [6].

b. J-T splitting of e_g orbitals producing $c/a > 1$ distortion.

c. Proposed quasi-static J-T version of $d^4 \leftrightarrow d^4$ that causes ferromagnetism through charge transfer into empty orbital states. It occurs in a rhombohedral structural phase that exists when the static cooperative distortions that cause orthorhombic phases are absent.

d. Conditions similar to those of b, but featuring charge transfer superexchange that promotes ferromagnetism.

where z is the number of nearest neighbors, J_{33}, $J_{34}(= J_{43})$, and J_{44} are the respective exchange constants of the individual magnetic pair interactions, and p_3 and p_4 are the probabilities of occurrence of S_3 and S_4 spins in any given site, and θ is the angle between spins, assumed to be uniform throughout the spin system. Since $p_3 = 1 - x$ and $p_4 = x$ for a random distribution, Equation (1) may be expressed as a function of x:

$$\begin{aligned} E_{ex} &= 2z\left[(1-x)^2 J_{33}S_3{}^2 + 2x(1-x)J_{34}S_3S_4 + x^2 J_{44}S_4{}^2\right]\cos\theta \quad , \\ &= 2zJS^2\cos\theta \quad , \end{aligned} \tag{2}$$

where $S = (1 - x)S_3 + xS_4$ is a weighted average spin value, and J is the corresponding average J_{ij} coefficient. The variation in E_{ex} with x may be inferred directly from the Curie/Néel temperature data [2], which register a peak $T_C > 300$ K at $x \approx 0.3$. A mathematical model is helpful in sorting out the contributions of the individual terms in Equation (2). To this end, the following empirical relation for J_{33} was constructed to simulate the vibronic J-T effects of the $Mn^{3+}O^{2-}Mn^{3+}$ interactions as a function of x:

$$J_{33} = J_{33}'\left\{1-\exp\left[-(x-x_0)/d_0\right]\right\}\left\{1-\exp\left[-(x_1-x)/d_1\right]\right\} \quad , \tag{3}$$

where x_0, x_1, d_0, and d_1 are parameters that may be structure and temperature dependent.

To relate E_{ex} to the Curie temperature, the standard expression $kT_C = 2zJS(S + 1)/3$ is employed to obtain:

$$kT_C = E_{ex}(S+1)/3S \quad . \tag{4}$$

Figure 6 shows plots of the calculations based on Equations (1) through (4) over the full range of x. To obtain a good fit with experiment the parameters were chosen to produce a $kT_C = 0.025$ eV (T_C = 300 K) with a peak at $x = 0.3$. From this exercise, $J_{33}' = 0.0022$ and $J_{34} = 0.0030$ eV. The value of $J_{44} = -0.00074$ eV is based on the reported Néel temperature of $T_N \approx 130$ K for $La^{3+}Ca^{2+}Mn^{4+}O_3$ [2], which would require a value of $E_{44} \approx 0.02$ eV at $x = 1.0$. [E_{ex} values above $x = 0.5$ are shown as a dashed line that is an artifact of the mathematical function of Equation (3) and are not intended to represent any quantitative physical reality in this regime.] It is therefore concluded that the relative importance of the terms in Equation (1) is heavily weighted towards the charge transfer E_{34} and E_{43} components in the vicinity of $x = 0.3$. Ferromagnetism in this system occurs because of the strength of the J_{34} interaction and because J_{33} is not antiferromagnetic in the range $0 \le x \le 0.5$ as normally expected.

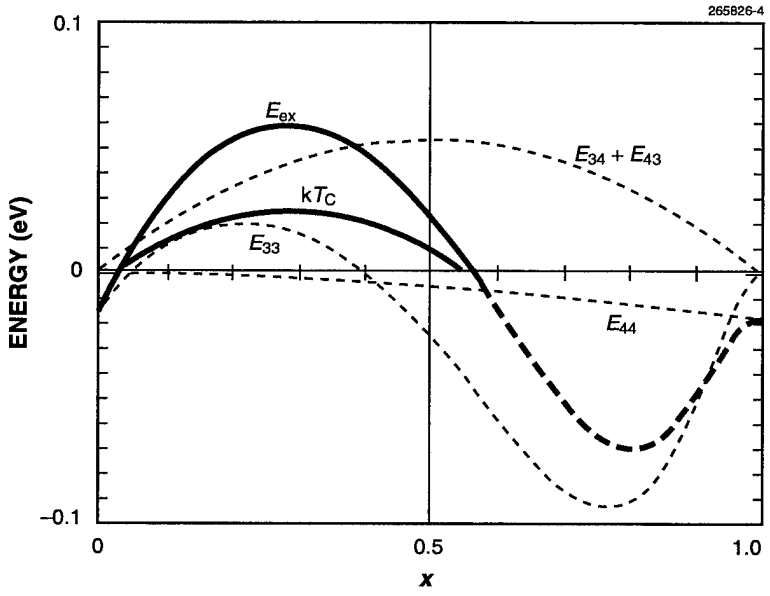

Figure 6. Calculated plot of E_{ex} and kT_C versus x, including estimated contributions of E_{33}, E_{44}, $E_{34}+E_{43}$. Parameter values used with exponential functions of Equation (3) are $x_0 = 0.1$, $d_1 = 0.4$, $x_1 = 0.7$, and $d_1 = 0.14$.

3.3 MAGNETIC MOMENT

Although the distribution of the Mn^{3+} and Mn^{4+} ions in these perovskites is likely to vary somewhat with composition and temperature, the conventional Weiss molecular field theory also may be applied to an individual spin S aligned in the direction of an applied magnetic field $\boldsymbol{H}$ and immersed in the exchange field H_{ex} of its own magnetic lattice. The combined gain in magnetic stabilization energy E_m may be expressed by a modification of Equation (2):

$$E_m = 2zJ\boldsymbol{S}\cdot\boldsymbol{S} + g\mu_B\boldsymbol{S}\cdot\boldsymbol{H} = 2zJS^2\cos\theta + g\mu_B SH \tag{5a}$$

$$= g\mu_B S(H_{ex} + H) \quad , \tag{5b}$$

where g is the gyromagnetic ratio (= 2), μ_B is the Bohr magneton in e.m.u., and $H_{ex} = NM$, M is the magnetic moment per mole of material, and N is the molecular or mean field coefficient expressed in moles/cm^3. N is related to the exchange constant J (in ergs) through

$$N = 2zJ / g^2\mu_B{}^2\mathcal{N} \quad , \tag{6}$$

where $\mathcal{N}$ is Avogadro's number.

The temperature and magnetic field dependence of the magnetic moment may then be described in the conventional manner by a Brillouin function B_S, which models the degree of spin collinearity, i.e., $\cos\theta$, according to

$$M(T,H) = M(0)B_S(y) \quad , \tag{7}$$

where $M(0) = g\mu_B S\mathcal{N}$ and $y = E_m(H)/kT$. From this theory, the Curie temperature with $H = 0$ may be calculated from the standard relation

$$T_C = 2zJS(S+1)/3k = g^2\mu_B{}^2 S(S+1)N\mathcal{N}/3k \quad . \tag{8}$$

In Figure 7, B_S is calculated by a numerical iterative procedure and plotted as a function of T for H values of 0 and 10 T. For $x = 0.3$, the N coefficient is 114 moles/cm^3 with a T_C value of 300 K. To illustrate further the sensitivity of B_S to external magnetic field, ΔB_S is also plotted. Although the behavior of the Brillouin function as $y \rightarrow 0$ may be simplified to $B_S(y) \approx (S + 1)y/3S$, the elegance of this approximation is quickly lost when $H \neq 0$. If $H \rightarrow 0$ is also assumed, however, the relation may be used to estimate the derivative of B_S with H by employing Equation (5) to express

$$B_S \approx \left(\frac{S+1}{3S}\right)\left(\frac{E_m}{kT}\right) = \frac{g\mu_B(S+1)[NM(0)B_S + H)]}{3kT} \quad , \tag{9}$$

which reduces to

$$B_S \approx \frac{g\mu_B(S+1)H}{[3kT - g\mu_B(S+1)NM(0)]} \quad . \tag{10}$$

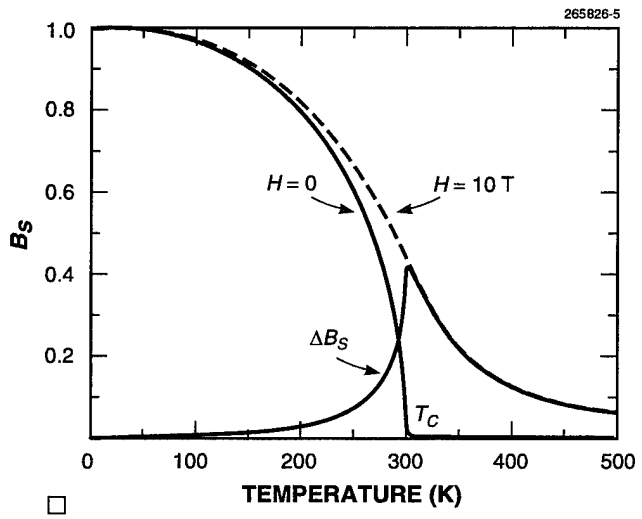

Figure 7. Calculated plots B_S and ΔB_S versus T for T_C = 300 K with H = 0 and 10 T.

After substitution of Equation (8) and differentiation with respect to H, the sensitivity of B_S to H becomes:

$$dB_S / dH \approx g\mu_B(S+1)/3k(T-T_C) \quad . \tag{11}$$

Inspecting Equation (11) reveals that a singularity exists at $T = T_C$ in a perfectly homogeneous material. A more realistic version might contain a ΔT_C term to represent a distribution width of T_C that arises from a spatial variation of N within the specimen. Since this situation would cause inhomogeneous broadening, a Gaussian-based model would be more appropriate. For analytical convenience, a simpler Lorentzian approach is adopted for this study. Equation (11) then becomes

$$dB_S / dH \approx g\mu_B(S+1)\mathcal{F}/3 \quad , \tag{12}$$

where $\mathcal{F} = [(T - T_C)^2 + (\Delta T_C)^2]^{-1/2}$. The effect of the ΔT_C term is usually observed as a tail on the B_S function above $T = T_C$. Where $T = T_C$, therefore, Equation (12) is reduced to:

$$\left(dB_S / dH\right)_{T=T_C} \approx g\mu_B(S+1)\mathcal{F}_C / 3\mathrm{k}T_C \quad , \tag{13}$$

where $\mathcal{F}_C = T_C/\Delta T_C$, the value of $\mathcal{F}$ at $T = T_C$. Since the uncertainty in a parameter that is inhomogeneously distributed is normally proportional to the magnitude of the parameter, it is reasonable to assume that $\mathcal{F}_C$ is a constant to a first-order approximation for any particular specimen. $\mathcal{F}_C$ may, therefore, serve as a parameter representing the degree of homogeneity.

3.4 INDIVIDUAL ELECTRON (S = 1/2) APPROXIMATION

The transfer of charge between Mn^{3+} and Mn^{4+} ions involves a single electron of spin s = 1/2. An alternative approach to the mean exchange field of this system is to consider the exchange energy as an algebraic sum of the contributions from the spins of individual orbital states.[1] In this case,

$$E_{ex} = 2zJS^2\cos\theta \approx 2zs^2\sum_k J_k^i\cos\theta_k \approx 2zs^2\cos\theta\sum_k J_k^i \quad ,$$
$$E_{ex} = 2zJ^i s^2\cos\theta \quad , \tag{14}$$

where J_k^i is the exchange constant and θ_k is the canting angle for the spins of orbital state k. It must also be pointed out that since the J^i constant is now defined as $b^2/2Us^2$ (instead of $J = b^2/2US^2$), the effective exchange constant and the molecular field coefficient increase by the factor $S(S+1)/s(s+1) \approx (4/3)S(S+1)$ to maintain the same T_C as defined by Equation (4) from the Brillouin function.

With this approximation, all the foregoing relations involving the Brillouin function may be employed, but with $S = s$ = 1/2. For this special case, $B_{1/2}(y) = \tanh(y)$. For comparison with Figure 6, $B_{1/2}$ for H = 0 and 10 T and $\Delta B_{1/2}$ are presented in Figure 8. As anticipated, N increases from 114 to 719 moles/cm^3 for the $B_{1/2}$ approximation. For the purpose of this analysis, this approximation provides a sharper transition at $T = T_C$ and will be shown to fit some of the magnetoresistance data more accurately.

---

[1] Recall from Equation (A-10) that the exchange energy of an individual d orbital may be equated to $b_k^2\cos\theta_k/2U_k$ for a pair of $Mn^{2+}(d^5)$ ions. Summed over the five d orbital states, therefore,

$$E_{ex} = z\left(b_{xy}{}^2\cos\theta_{xy}/2U_{xy} + b_{xz}{}^2\cos\theta_{xz}/2U_{xz} + b_{yz}{}^2\cos\theta_{yz}/2U_{yz}\right)$$
$$+ z\left(b_{z^2}{}^2\cos\theta_{z^2}/2U_{z^2} + b_{x^2-y^2}{}^2\cos\theta_{x^2-y^2}/2U_{x^2-y^2}\right)$$
$$\approx z\left(b_{xy}{}^2 + b_{xz}{}^2 + b_{yz}{}^2 + b_{z^2}{}^2 + b_{x^2-y^2}{}^2\right)(\cos\theta/2U) \quad ,$$

where b_k, θ_k, and U_k represent the transfer integral, canting angle, and ionization energy of the orbital state k, respectively.

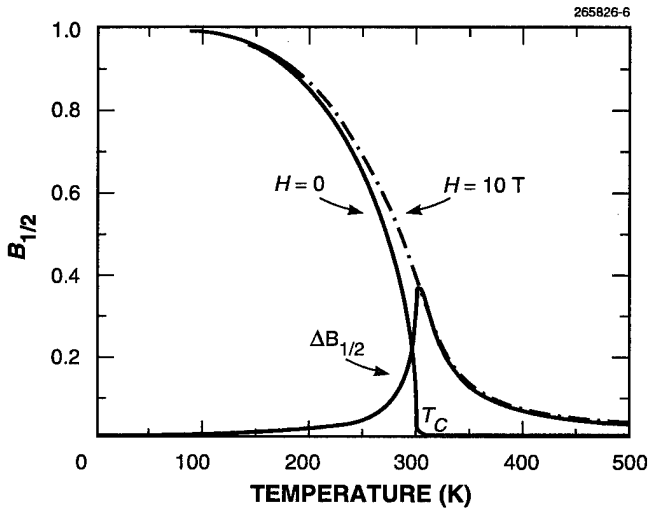

Figure 8. Calculated plots $B_{1/2}$ and $\Delta B_{1/2}$ versus T for T_C = 300 K with H = 0 and 10 T.

4. MAGNETORESISTIVE PROPERTIES OF $(RE^{3+}A^{2+})MnO_3$

4.1 RESISTIVITY VERSUS TEMPERATURE AND MAGNETIC FIELD

The electrical conductivity of mixed-valence oxides obeys the standard relation for mobility-activated semiconduction [11–13],

$$\sigma = ne(eD/\mathrm{k}T)\exp(-E_{\mathrm{hop}}/\mathrm{k}T) \quad , \tag{15}$$

where the factor $(eD/\mathrm{k}T)$ is the Einstein diffusion mobility, n is the carrier density, and D the diffusion constant that equals the ratio of the square of the hop distance to the carrier lifetime d^2/τ. In previous studies of the normal state of the cuprate superconductors [14,15], this relation was refined and expressed as a resistivity:

$$\rho = C(\mathrm{k}T)[(1-x)/x]\exp(E_{\mathrm{hop}}/\mathrm{k}T) \quad , \tag{16}$$

where the effective number of carriers per formula unit $x(1-x) = nV$, V is the volume of a formula unit ($\sim a^3$) based on lattice parameter a (= 4 A), and $C = V/e^2 d_{\mathrm{min}}{}^2 \nu_{\mathrm{hop}}$. The hopping frequency $\nu_{\mathrm{hop}}(= 1/\tau)$ is equated to the Debye frequency $\nu_{\mathrm{D}} = (\mathrm{k}/h)\Theta_{\mathrm{D}} \approx 5 \times 10^{12}$ Hz for a Debye temperature $\Theta_{\mathrm{D}} \approx 250$ K. The $(1-x)$ factor in the numerator of Equation (2) arises from a correction to the effective hop distance d ($\propto a$), which increases with x according to $d_{\mathrm{min}}/(1-x)$. By Equation (2), ρ passes through a minimum at $T = E_{\mathrm{hop}}/\mathrm{k}$ and assumes a metallic slope that approaches the linear function $C(\mathrm{k}T)[(1-x)/x]$.

The most influential parameter in Equation (16) is the activation energy E_{hop} that appears in the Boltzmann exponential factor. The principal source of E_{hop} is the reduction in stabilization energy [15,16] of the electron carrier in the e_g orbitals that covalently link the Mn^{3+} and Mn^{4+} ions. This loss in binding energy represents the additional (thermal) energy required to effect the carrier transfer and occurs because of spin canting. Since B_S is the z-axis projection of spins within a cone of half-angle θ, it also represents the average angle between a spin and the direction of the exchange field in which it resides. Consequently, $\cos\theta$ may be represented by B_S in Equation (A-12), and the spin canting effect on the binding energy can now be expressed as a function of temperature and magnetic field.

The total activation energy may then be expressed according to Equation (A-14) as:

$$E_{\mathrm{hop}} = E_{\mathrm{hop}}{}^0 + E_{\mathrm{hop}}{}^{ex}\left[1 - B_S(T,H)\right] \quad , \tag{17}$$

where $E_{\mathrm{hop}}{}^0$ is the polaron trap energy at temperatures below Θ_{D} (typically < 0.01 eV for the high-T_c cuprates and here chosen as 0.004 eV [17]), and $E_{\mathrm{hop}}{}^{ex}$ (~ 0.1 eV) is the magnetic exchange contribution that reaches its full value when the spins become disordered at $T > T_c$. Although $E_{\mathrm{hop}}{}^0$ may have little or no influence at temperatures far below T_C, it is included here partly for convenience and partly to reflect a worst-case situation. If the dominant conduction mechanism is polaronic in this regime, $E_{\mathrm{hop}}{}^0$ could be ignored. The suitability of this estimate for $E_{\mathrm{hop}}{}^{ex}$ and its relation to the exchange stabilization energy of a carrier in its trap may be justified by equating it to that portion of the total exchange energy

that is contributed by the electron transfer between an ion and its surrounding neighbors. Therefore,

$$E_{\text{hop}}{}^{ex} \approx 2zJ_{34}S_3S_4 = 0.106 \text{ eV} \quad , \tag{18}$$

for $z = 6$, $J_{34} = 0.0030$ eV, $S_3 = 2$, and $S_4 = 3/2$.

In Figures 9 and 10, which use the B_S and $B_{1/2}$ approximations, respectively, ρ versus T data of Li et al. [18] for a composition estimated as $(La^{3+}{}_{0.77}Ca^{2+}{}_{0.23})MnO_3$ subjected to H fields of 0, 1, 3, 5, and 14 T are fitted by curves generated from Equation (16). Except for the $H = 0$ curve, which did not reach its full peak probably due to the inhomogeneously broadened tail of the M versus T curve, theory and data are in reasonably good agreement. The discrepancies are largely the result of the molecular field approximation which represents the z-axis projection of the combined magnetic moment from all of the spins that occupy a cone of average half angle θ. Any difference between θ and the average canting angle between neighboring S_3 and S_4 spins could account for the relatively small disagreement between theory and measurement in the metallic region below T_C. In Figures 9 and 10, $C = 7.2$ and 6 mΩcm/eV, respectively, and $E_{\text{hop}}{}^{ex} = 0.1$ eV. For all subsequent computations, $C = 6$ mΩcm/eV is used.

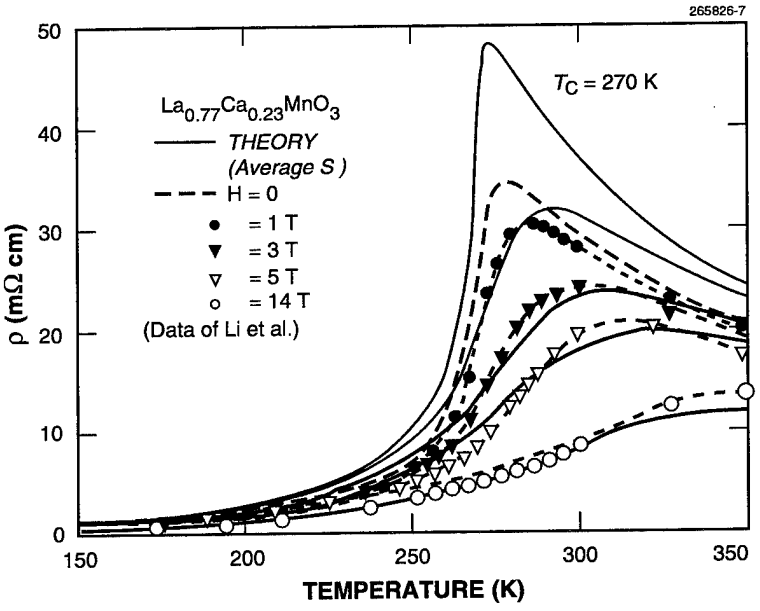

Figure 9. Comparison of B_S approximation theory with experiment for ρ versus T with H = 0, 1, 3, 5, and 14 T. Data are from Budnick et al. [18].

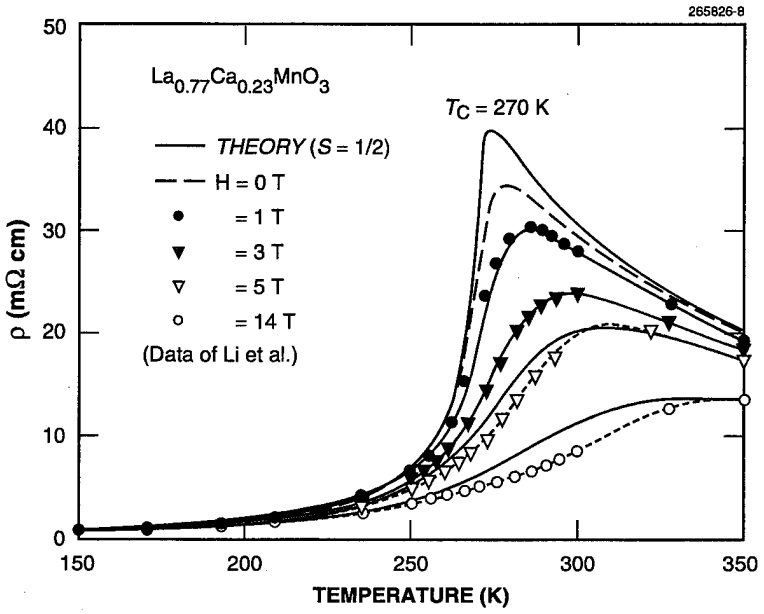

Figure 10. Comparison of the $B_{1/2}$ approximation theory with ρ versus T data of Figure 9.

In Figures 11 and 12, respectively, example curves of ρ from the B_S and $B_{1/2}$ approximations are plotted as functions of T with H values of 0, 0.1, 1, and 10 T for Curie temperatures at 100, 200, and 300 K.[2] since E_{hop}^{ex} is a constant of the transfer ions, the peaks of ρ at $H = 0$ should theoretically touch the $(kT)\exp(E_{hop}/kT)$ envelope at the appropriate T_C values. From these results, the magnitude of the anomalous increase in ρ at T_C is shown to increase by almost four orders of magnitude between 300 and 100 K. The ρ_{max} ($H = 0$) values listed in Table 3 are greater by about 50% than the measured values reported in the literature, which are typically ~ 10^2 Ωcm at $T_C = 100$ K. The computed value of ρ_{max} = 145 Ωcm for $T_C = 100$ K at $H = 0$ approaches an upper limit of the $(kT)\exp(E_{hop}/kT)$ envelope, which might be expected for an ideal material.

The results from the $B_{1/2}$ approximation depart from those found by the B_S approximation mainly in the subtle differences in curve contours near T_C. In either case, it was observed that ρ_{max} occurred at T slightly greater than T_C because of the Brillouin function tail above T_C. This tail results from the iterative mathematical procedure used to solve for B_S. In actual measurements, the ρ_{max} should also appear offset from T_C because a tail in $M(T)$ occurs above T_C due the inhomogeneities mentioned earlier.

[2] Note that the curves in these figures are extended to $T = 0$, where ρ rises sharply because of the assumed residual activation energy $E_{hop}^{0} = 0.004$ eV. In reality, the hopping mechanism may be dominated by polaronic "tunneling" at these lowest temperatures and the metallic region would theoretically reach $T = 0$, where ρ would also approach zero. Only at higher temperatures where T approaches Θ_D, does b_p decrease sufficiently for activated hopping to compete with polaronic tunneling (see Footnote 3).

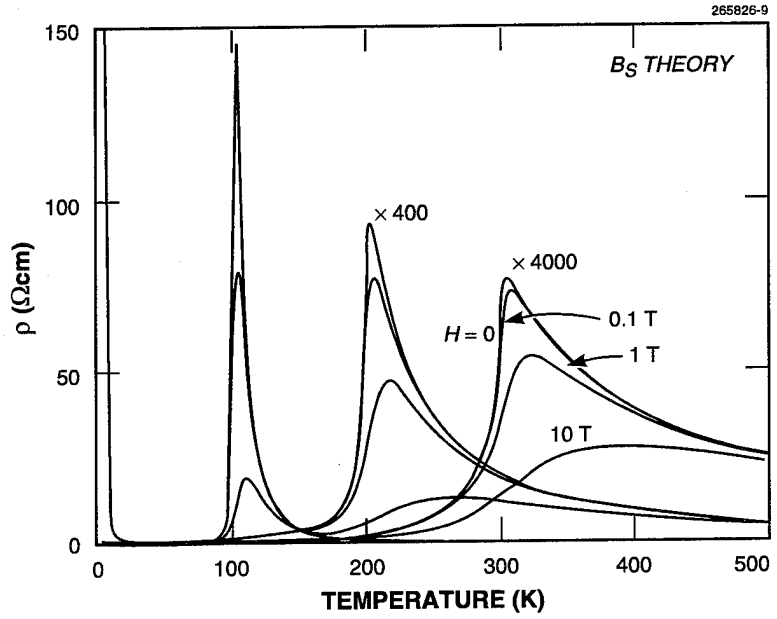

Figure 11. Predicted plots of ρ versus T by the B_S approximation for T_C values of 100, 200, and 300 K. Magnetic field strengths are H = 0, 0.1, 1, and 10 T.

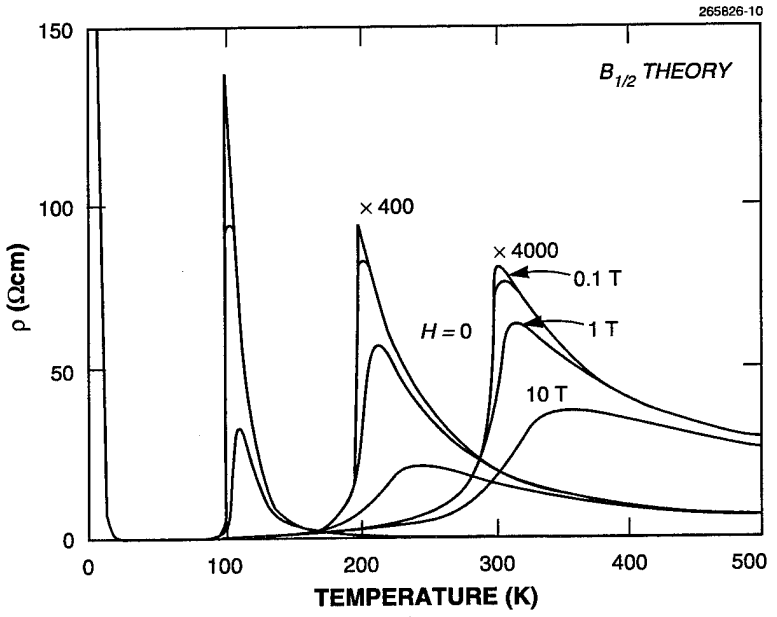

Figure 12. Predicted plots of ρ versus T by the $B_{1/2}$ approximation for T_C values of 100, 200, and 300 K. Magnetic field strengths are H = 0, 0.1, 1, and 10 T.

TABLE 3

Parameter Values from Figure 10[a]

T_C (K)	x –	N (moles/cm^3)	ρ_{max}[b] (H = 0) (Ωcm)	(1/ρ)Δρ/ΔH (ΔH = 1 Oe) (Oe^{-1})
77	0.04	26	4770	-4.7×10^{-3}
100	0.05	34	145	-3×10^{-3}
200	0.15	71	0.233	-1×10^{-3}
300	0.30	114	0.020	-2×10^{-4}

a. For these calculations, C = 6 Ωcm/eV, E_{hop}^{0} = 0.004 eV, and E_{hop}^{ex} = 0.1 eV.

b. ρ_{max} occurs at a value of T that is slightly larger than T_C because of the "paramagnetic" tail of the M versus T curve as $M \rightarrow 0$.

Comparison of the B_S theory with experiment with T_C = 110 K for ρ as a function of H is also shown in Figure 13 for a $La_{0.67}Ca_{0.33}MnO_y$ film reported by Chen et al. [19]. The magnitude of ρ is fitted with a scale factor of only 1.3 applied to the calculations, but the difficulty in constructing the wings of the curve is seen more clearly. To use this model for prediction purposes, the M versus T curve must have a sharper decrease as $T \rightarrow T_C$.

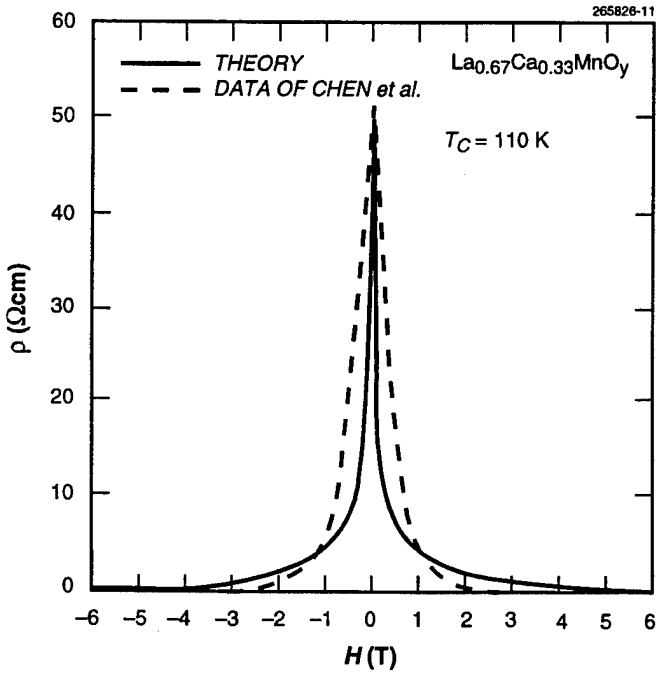

Figure 13. Comparison of theory with experiment for ρ versus H (B_S approximation) from a $La_{0.67}Ca_{0.33}MnO_y$ film with T_C = 110 K. Data are from Chen et al. [19].

4.2 SENSITIVITY OF RESISTIVITY TO MAGNETIC FIELD

Consistent with these effects are the corresponding increases in the sensitivity of ρ to applied H with decreasing T_C values as anticipated from the previous dB_S/dH analysis in the limit as $H \rightarrow 0$ from Equations (9) through (12).

From Equations (12), (16), and (17), it may be readily determined that $d\rho/dH$ at $T = T_C$ is proportional to $(1/T_C)\exp(E_{hop}/kT_C)$, and

$$(1/\rho)d\rho/dH = -g\mu_B(S+1)E_{hop}{}^{ex}\mathcal{F}_C/3(kT_C)^2 \quad . \tag{19}$$

Equation (19) states that $(1/\rho)d\rho/dH$ is inversely proportional to $T_C{}^2$, which is suggested by the results listed in Table 3 from the B_S approximation at $T = T_C$. Relative estimates of $(1/\rho)\Delta\rho/\Delta H$ for the $H \rightarrow 0$ limit were computed for $\Delta H = 1$ Oe^{-1} as -4.7×10^{-3}, -3×10^{-3}, -1×10^{-3}, and -2×10^{-4} Oe^{-1} at $T_C = 77$, 100, 200, and 300 K, respectively. The corresponding $\Delta\rho/\rho$ values are plotted in Figure 14 as a function of H on a $\log_{10}$ scale. (In this exercise, there was no attempt to introduce a value for $\mathcal{F}_C$. Finite values at the $T = T_C$ singularity were simply the result of an artifact related to the degree of precision used in the Brillouin function iteration procedure.)

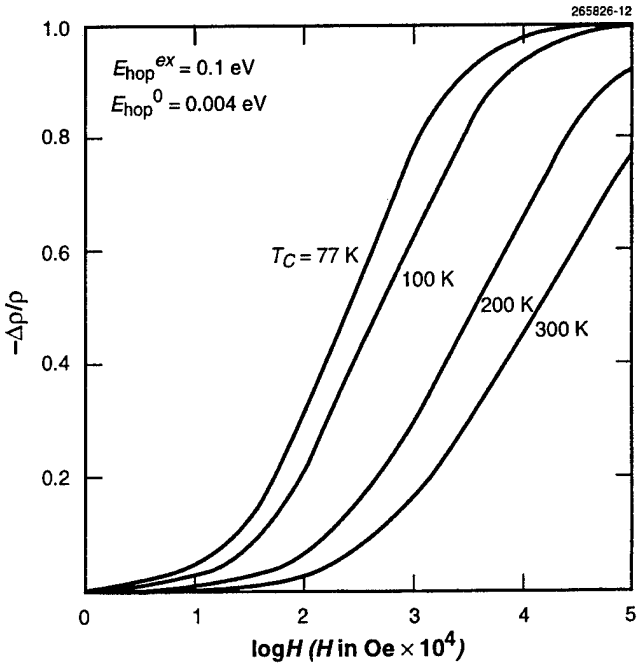

Figure 14. Variation of $\Delta\rho/\rho$ with $\log_{10}H$ for T_C = 77, 100, 200, and 300 K using the B_S approximation.

5. $Mn^{3+(4+)}$ AND $Cu^{2+(3+)}$ CHARGE TRANSFER

Metallic conductivity in transition-metal oxides in which significant magnetic exchange energy can be present may also occur in select situations where the minority transfer ion is in a zero-spin state ($S = 0$). A remarkable example of this situation is seen in p-type $Cu^{2+}(d^9)$-O^{2-}-$Cu^{3+}(d^8, ls)$ [ls = low spin] and n-type $Cu^{2+}(d^9)$-O^{2-}-$Cu^{1+}(d^{10})$ configurations, as well as in 180° bonds of the perovskite structure. For the Cu^{3+} ion, the $S = 0$ state arises from an ls configuration (see Figure 2) that occurs because of a large splitting of the e_g doublet [20]. Here the splitting of $d_{x^2-y^2}$ and d_{z^2} exists naturally as a result of the tetragonal/orthorhombic symmetry of the layered-type perovskites and not necessarily from a J-T effect required to create the splitting in the manganites. Unlike the case where ferromagnetism, induced as a byproduct of spin-polarized electron transfer in the $Mn^{3+(4+)}$ combinations, eliminates the exchange contribution E_{hop}^{ex} to the activation energy, the involvement of $S = 0$ ions removes the internal polarization exchange energy and therefore renders moot any Hund's Rule considerations. In addition, charge transfer from these mobile nonmagnetic ions of the polaron causes local breakdowns of the antiferromagnetic couplings and can eventually reduce the Néel temperature T_N to zero by causing the spin alignment frustration to spread throughout the entire lattice [16].

As presented in Figure 15, the polaronic hole carriers created by a zero-spin Cu^{3+} ions of concentration $x < 0.08$ in $La_{2-x}Sr_xCuO_4$ would be more than sufficient to eliminate the magnetic order among the sites immediately surrounding the fixed negative charge represented by the Sr^{2+} dopant, by establishing a ring of mobile carriers (as in Figure 2), and then to frustrate through spin canting the regions beyond these lowest energy polaron sites. As a consequence, ferromagnetic interactions are neither present nor necessary for this covalent charge transfer to occur. A list of possible $S = 0$ candidates among the $3d^n$ series and a diagram for the occupancies of the transfer orbitals $d_{x^2-y^2}$ and d_{z^2} for the different cases may be found in Dionne [15]. The metallic resistivity behavior of $La_{2-x}Sr_xCuO_4$ is demonstrated in Figure 16. For the fitting of these data [21], $C = 16$ mΩcm/eV, which is larger than that for $La_{1-x}Ca_xMnO_3$ because of 50% higher lattice volume fraction occupied by B sites and the large angle grain boundaries in these bulk ceramic specimens. For textured films of $YBa_2Cu_3O_7$, the value of C is 9 mΩcm/eV [14,15], which scales closely with the value of 6 mΩcm/eV used for $La_{0.77}Ca_{0.23}MnO_3$ in Figures 9 and 10.

The influence of magnetic exchange on the $Cu^{2+(3+)}$ conductivity in the presence of rare-earth ions occupying the A sublattice is shown dramatically in Figure 17, where the data of George et al. [22] reveal the virtual absence of an activation energy for the nonmagnetic La compound. In all the others, antiferromagnetic interactions deter the formation of large polarons that are necessary for the coherent activationless charge transfer of superconductivity. In the La compound the presence of only 5% zero-spin Cu^{3+} is sufficient to frustrate the antiferromagnetic ordering, create the metallic phase of the superconducting state, and allow the onset of superconductivity (the $T_N, T_c = 0$ condition [15,16]) as shown in Figure 18.

In summation, the mixed-valence manganites and cuprates are metallic if the contribution to the hopping activation energy from antiferromagnetic exchange is compromised. $La_{1-x}Ca_xMnO_3$ is metallic for $x < 0.5$ because of the occurrence of ferromagnetism that results from delocalization exchange between partially filled e_g orbital states. The existence of a spontaneous magnetic moment, however, also

precludes the possibility of superconductivity. $La_{2-x}Sr_xCuO_4$ and other high-T_c cuprates are metallic because the zero-spin Cu ions remove the possibility of magnetic exchange trapping and frustrate any antiferromagnetic order above a concentration threshold of only a few percent. In both cases, large polarons may form at low temperatures, in one case producing a condition from which a magnetoresistance anomaly may occur at the Curie temperature, and in the other, making possible the covalent charge transfer between $S = 1/2$ and $S = 0$ ions that is a feature of high-T_c superconductivity.

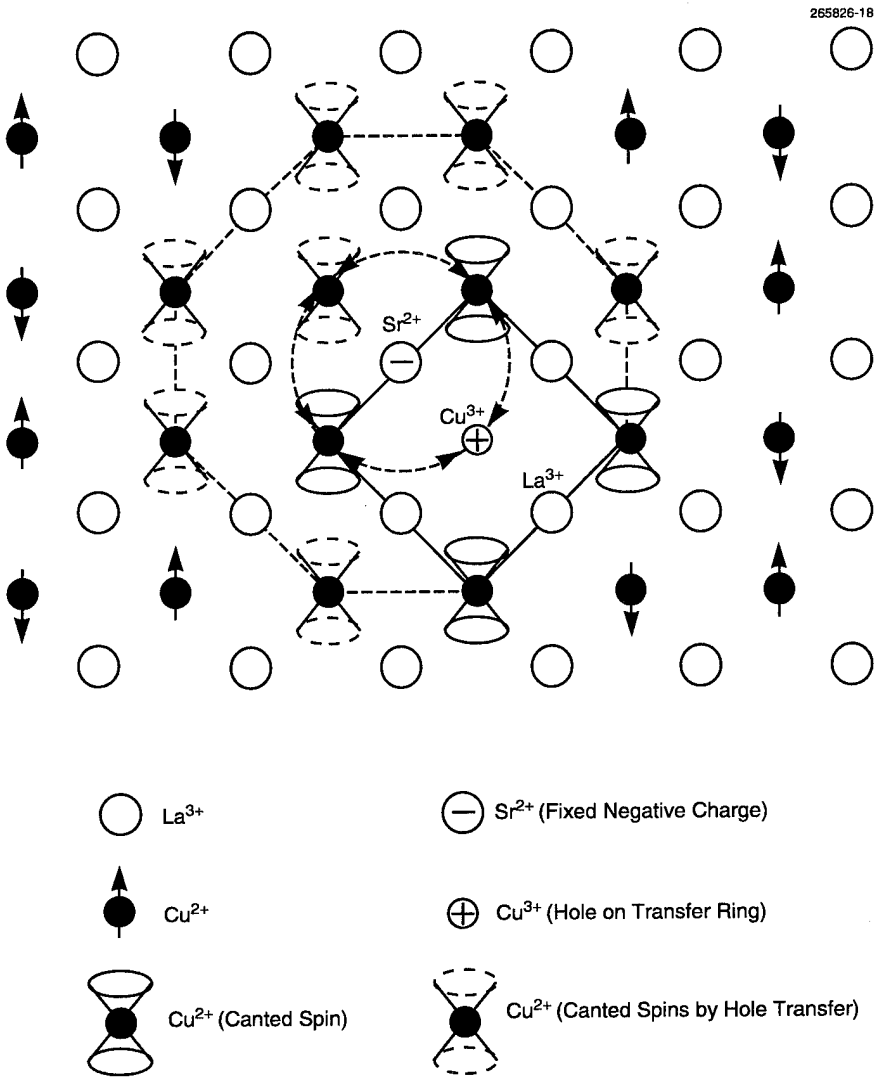

Figure 15. Origin of antiferromagnetic frustration caused by zero-spin Cu^{3+} ions in $La_{2-x}Sr_xCuO_4$. Breakdown in ordering can occur with only 1 out of 12 ($x \approx 0.08$) $S = 0$ sites in the Cu^{2+} sublattice in the region surrounding an Sr^{2+} impurity that acts as a fixed negative charge. Note that the Cu^{3+} hole can transfer around the inner ring in the manner of the model in Figure 2, bringing the canted spins of the four Cu^{2+} with it.

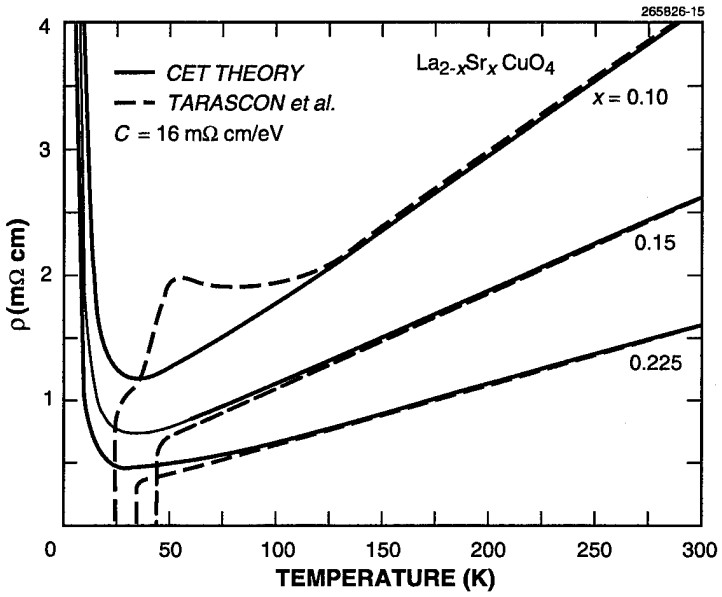

Figure 16. Comparison of theory with measured ρ versus T for the $La_{2-x}Sr_xCuO_4$ system case. Data are from Tarascon et al. [21].

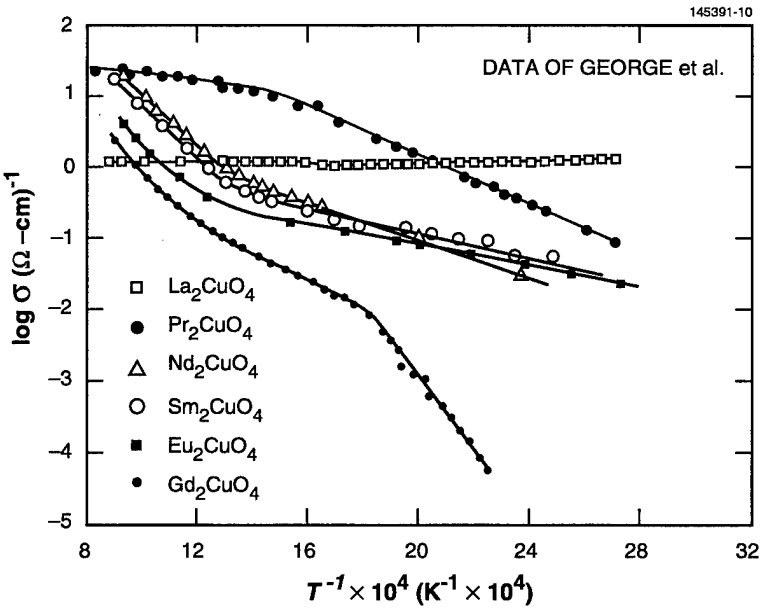

Figure 17. Conductivity σ data as a function of temperature, showing the influence on the activation energies from RE ion exchange interactions with Cu^{2+} ions in a $(RE)_2CuO_4$ series. Note the absence of E_{hop}^{ex} in the La_2CuO_4 case. Data are from George et al. [22].

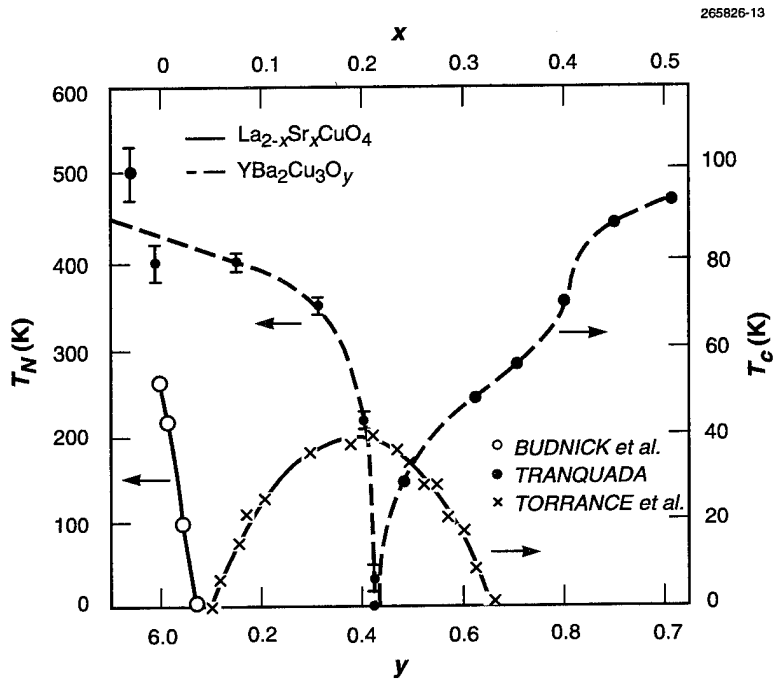

Figure 18. Experimental verification of the magnetic frustration requirement prior to the onset of superconductivity in $La_{2-x}Sr_xCuO_4$ and $YBa_2Cu_3O_y$ systems. Data from Budnick et al. [23], Tranquada [24], and Torrance et al. [25].

6. DISCUSSION AND CONCLUSIONS

The anomalous magnetoresistance effect at the Curie temperature in the $(RE^{3+}_{1-x}A^{2+}_{x})MnO_3$ series results from ferromagnetism that is caused by kinetic exchange between Mn^{3+}-Mn^{4+} ions and the resonating charge transfer of the vibronic J-T effect between Mn^{3+}-Mn^{3+} ions. This combination eliminates the magnetic exchange trap and causes a metallic resistivity through covalent (polaron tunneling) transfer. The evidence also lends support to the theory that the metallic behavior of the superconducting cuprates is caused by the absence of an antiferromagnetic trap, in that case due to $S = 0$ Cu^{3+} ions. The sharp increase in E_{hop} that causes the magnetoresistance occurs with the transition from ferromagnetic to random ordering, as the charge transfer between e_g orbitals becomes impeded by spin misalignments above T_C.

Measured data can be readily modeled by the traditional Brillouin-Weiss molecular field theory. Except for the difficulty in accurately computing the tail of the Brillouin function at T_C, which broadens the resistivity singularity at the transition between metallic ($T < T_C$) and insulating ($T > T_C$) regimes, the measurements may be fitted with reasonably good accuracy as functions of both T and H. In general, the Brillouin curve lies below those obtained by experiment and would tend to predict less severe increases in dB_S/dH. For these systems with multivalent magnetic ions that are easily mobile through electron transfer, there is the added uncertainty of ionic ordering that may change with temperature, as pointed out by Jonker and Van Santen [2].

The principal insights gained from this interpretation of the phenomenon are:

1. The key to the magnetoresistance is the presence of ferromagnetism that is caused by a combination of charge transfer exchange between Mn^{3+}-O^{2-}-Mn^{4+} and the vibronic J-T effect between Mn^{3+}-O^{2-}-Mn^{3+}. The magnetic condition may be exclusively a property of d^4 and d^3 covalently linked cations in octahedral sites through 180° bonds.

2. The resistivity maximum $\rho_{max} \sim [(1 - x)/x]\,(kT_C)\exp(E_{hop}/kT_C)$ at $H = 0$ and occurs at the dB_S/dH peak slightly above $T = T_C$.

3. The maximum of the magnetoresistance effect $\Delta\rho/\Delta H$ occurs at the Curie temperature, which may appear slightly below the temperature at the dB_S/dH peak, where the resistivity also reaches ρ_{max}. The difference depends on the extent of the paramagnetic tail of the magnetic moment above T_C.

4. The magnitude of $\Delta\rho/\Delta H$ at $T = T_C$ is mainly determined by the factor $(1/kT_C)\exp(E_{hop}/kT_C)$ and can increase by orders of magnitude with decreasing T_C. An additional dependence on carrier concentration x enters through its influence on T_C, as illustrated in Figure 6.

5. The magnitude of the relative magnetoresistance effect $(1/\rho)\Delta\rho/\Delta H$ at $T = T_C$ is approximately determined by the factor $1/T_C^2$. As indicated by the results in Table 3, the relative sensitivity should suffer by only a factor of ~20 for an increase in T_C from 77 to 300 K.

6. Both $\Delta\rho/\Delta H$ and $(1/\rho)\,\Delta\rho/\Delta H$ decrease with increasing T_C of the material. The extent of the paramagnetic tail characterized by ΔT_C should be as small as possible for maximum sensitivity.

7. The value of E_{hop}^{ex} is determined by the transfer energy $2zJ_{34}S_3S_4$, which is estimated at 0.106 eV in Equation (18) based on the analysis of the magnetic properties. This conclusion is supported by the fact that a single value of $E_{hop}^{ex} = 0.1$ eV was used for all these computations, which have produced good agreement with the measured results reported in the literature.

8. Since T_C is expressed by Equation (8), $E_{hop}^{ex}/kT_C \sim 6J_{34}S_3S_4/JS(S+1)$ and is therefore mainly dependent only on the magnetic exchange properties of the system, which are dominated by the $2J_{34}S_3S_4$ contributions.

To exploit the magnetoresistance effect by increasing the E_{hop}/kT_C factor, it would be desirable to raise $E_{34} \sim 2zJ_{34}S_3S_4$ without influencing the overall exchange energy, particularly at 300 K where the $\Delta\rho/\Delta H$ anomaly falls by orders of magnitude from the dramatically large values at low temperatures. However, since E_{34} is also the dominant part of the ferromagnetic exchange energy through its charge transfer feature, there is little flexibility to enhance $\Delta\rho/\Delta H$ in this particular materials system. Any attempt to increase E_{hop}^{ex} by altering the magnetic trap energy, e.g., by increasing the transfer integral b_t through the substitution of larger cations (or anions), would also raise T_C. The most practical approach for optimizing this effect might be simply to design an ideal cation distribution to ensure a minimum ΔT_C.

REFERENCES

1. S. Jin, T.H Tiefel, M. McCormack, R.A. Fastnacht, R. Ramesh, and L.H. Chen, "Thousandfold change in resistivity in magnetoresistive La-Ca-Mn-O films," *Science* **264**, 413 (1994).
2. G.H. Jonker and J.H. Van Santen, "Ferromagnetic compounds of manganese with perovskite structure," *Physica* **XVI**, 337 (1950).
3. J.H. Van Santen and G.H. Jonker, "Electrical conductivity of ferromagnetic compounds of manganese with perovskite structure," *Physica* **XVI**, 599 (1950).
4. P.W. Anderson, "New approach to the theory of superexchange interactions," *Phys. Rev.* **115**, 2 (1959).
5. J. Kanamori, "Superexchange interaction and symmetry properties of electron orbitals," *J. Chem. Phys. Solid.* **10**, 87 (1959).
6. J.B. Goodenough, *Magnetism and the Chemical Bond*, New York: Interscience Publishers, John Wiley (1963).
7. T. Holstein, "Studies of polaron motion," *Ann. Phys.* **8**, 325 (1959).
8. J.B. Goodenough, A. Wold, N. Menyuk, and R.J. Arnott, "Relationship between crystal symmetry and magnetic properties of ionic compounds containing Mn^{3+}," *Phys. Rev.* **124**, 373 (1961).
9. C. Zener, "Interaction between the *d*-shells in the transition metals. II. Ferromagnetic compounds of manganese with perovskite structure," *Phys. Rev.* **82**, 403 (1951).
10. P.-G. de Gennes, "Effects of double exchange in magnetic oxides," *Phys. Rev.* **118**, 141 (1960).
11. J.B. Goodenough, "Metallic oxides," *Prog. Solid State Chem.* **5**, 145 (1972).
12. R.R. Heikes and W.D. Johnston, "Mechanisms of conduction in Li-substituted transition metal oxides," *J. Chem. Phys.* **26**, 582 (1957).
13. R.J.D. Tilley, *Defect Crystal Chemistry and Its Applications*, Glasgow and London: Blackie, Chap. 6 (1987).
14. G.F. Dionne, "Resistivity of multiphase high-T_C superconductors," *J. Appl. Phys.* **69**, 4883 (1991).
15. G.F. Dionne, "Covalent electron transfer theory of superconductivity," MIT Lincoln Laboratory Technical Rep. 885 (19 June 1992), DTIC AD-A253975.
16. G.F. Dionne, "Magnetic frustration in high-T_C superconductors," *J. Appl. Phys.* **69**, 5194 (1991).
17. G.F. Dionne, "Temperature dependence of large polaron superconductivity," MIT Lincoln Laboratory Technical Rep. 1024 (18 July 1995), DTIC AD-A297287.
18. Y-Q. Li, J. Zhang, S. Pombrik, S. DiMascio, W. Stevens, Y.F. Yan, and N.P. Ong, "*In-situ* single-liquid-source metalorganic chemical vapor deposition of (La,Ca)MnO_3 giant magnetoresistive films," *J. Mater. Res.* **10**, 2166 (1995).

19. L.H. Chen, S. Jin, T. Tiefel, R. Ramesh, and D. Schurig, "Large magnetoresistance in La-Ca-Mn-O films," *IEEE Trans. Magn.* **31**, 3912 (1995).

20. J.B. Goodenough, G. Demazeau, M. Pouchard, and P. Hagenmüller, "Sur une nouvelle phase oxygénée du cuivre +III:$SrLaCuO_4$," *J. Solid State Chem.* **8**, 325 (1973).

21. J.M. Tarascon, L.H. Greene, W.R. McKinnon, G.W. Hull, and T.H. Geballe, "Superconductivity at 40 K in the oxygen-defect perovskites $La_{2-x}Sr_xCuO_{4-y}$," *Science* **235**, 1373 (1987).

22. A.M. George, I.K. Gopalakrishnan, and M.D. Karkhanavla, "Electrical conductivity of Ln_2CuO_4 compounds," *Mater. Res. Bull.* **9**, 721 (1974).

23. J.I. Budnick, B. Chamberland, D.P. Yang, C. Neidermayer, A. Golnik, E. Recknagel, M. Rossmanith, and A Weidinger, "Dependence of the Néel temperatures of La_2CuO_4 on Sr-doping studied by muon spin rotation," *Europhys. Lett.* **5**, 651 (1988).

24. J.M. Tranquada, "Antiferromagnetism in $YBa_2Cu_3O_{6+x}$," *J. Appl. Phys.* **64**, 6071 (1988).

25. J.B. Torrance, Y. Tokura, A.I. Nazzal, A. Bezinge, T.C. Huang, and S.S.P. Parkin, "Anomalous disappearance of high-T_C superconductivity at high hole concentration in metallic $La_{2-x}Sr_xCuO_4$," *Phys. Rev. Lett.* **61**, 1127 (1988).

26. G.W. Pratt, Jr., "Antiferromagnetism," *Phys. Rev.* **97**, 926 (1955).

27. G.F. Dionne, "New two-fluid superconduction model applied to penetration depth and microwave surface resistance," *IEEE Trans. Appl. Supercond.* **3**, 1465 (1993).

APPENDIX
ORIGINS OF THE ACTIVATION ENERGY

A carrier occupying a lattice trap may be described in terms of a classical Boltzmann approximation to the Fermi-Dirac function provided that the carrier density is low enough to be considered in a localized state regime. The key parameter in determining the density of carriers in this limit is therefore the activation energy for charge transport, defined here as E_{hop}. The process of transporting charge in a mixed-valence transition-metal oxide involves two steps:

Polaron Stabilization Energy. In the simplest case of a trapped charge, called a polaron at low temperatures, it is assumed that the trap is of elastic (hence electrostatic) origin with the carrier tethered to a nearby fixed charge. It is also assumed that there are no spin polarization limitations and that the only restriction on the polaron mobility is the electrostatic forces binding it to its source in the lattice. The solution is worked out in terms of the difference in electrostatic energy ΔE_p between the two lattice sites, and the temperature-dependent width of the polaron carrier band b_p that also represents the transport transition probability between polaron states ψ_{p1} and ψ_{p2}.[3]

The standard secular equation for the situation in Figure A-1(a) is

$$\begin{vmatrix} \mathcal{H}_{11} - E & \mathcal{H}_{12} \\ \mathcal{H}_{12} & \mathcal{H}_{22} - E \end{vmatrix} = \begin{vmatrix} E_{p1} - E & b_p \\ b_p & E_{p2} - E \end{vmatrix} = 0 \quad , \tag{A-1}$$

and the straightforward solution of the resulting quadratic equation is

$$E_{\pm} = E_F \pm \frac{\sqrt{\Delta E_p{}^2 + 4 b_p{}^2}}{2} \quad , \tag{A-2a}$$

and

$$\chi_{-} = C_1 \Psi_{p1} + C_2 \Psi_{p2} \tag{A-2b}$$

---

[3] b_p is reduced by vibronic (orbit-lattice) coupling that produces a temperature-dependent narrowing of the electronic half bandwidth b_t given by an expression $b_p = b_t \exp[-\gamma \coth(\Theta_D/2T)$ that ranges from b_t at $T \rightarrow 0$ to $b_t \exp[-\gamma(2T/\Theta_D)]$ when $2T >> \Theta_D$. The parameter $\gamma \sim 50/K_{opt}{}^2$, and would be ~ 1 for transition-metal oxides with an optical dielectric constant K_{opt} in the 6-to-10 range. According to Holstein [7], when $T \geq \Theta_D/2$, the decrease in b_p causes a reduction in polaron tunneling and allows electron hopping to become the dominant conduction mechanism.

for the bonding state, where

$$C_1 = \left(1/\sqrt{2}\right)\left[\frac{\sqrt{\Delta E_p{}^2 + 4b_p{}^2} + \Delta E_p}{\sqrt{\Delta E_p{}^2 + 4b_p{}^2}}\right]^{1/2} \qquad \text{(A-2c)}$$

$$C_2 = \left(1/\sqrt{2}\right)\left[\frac{\sqrt{\Delta E_p{}^2 + 4b_p{}^2} - \Delta E_p}{\sqrt{\Delta E_p{}^2 + 4b_p{}^2}}\right]^{1/2}$$

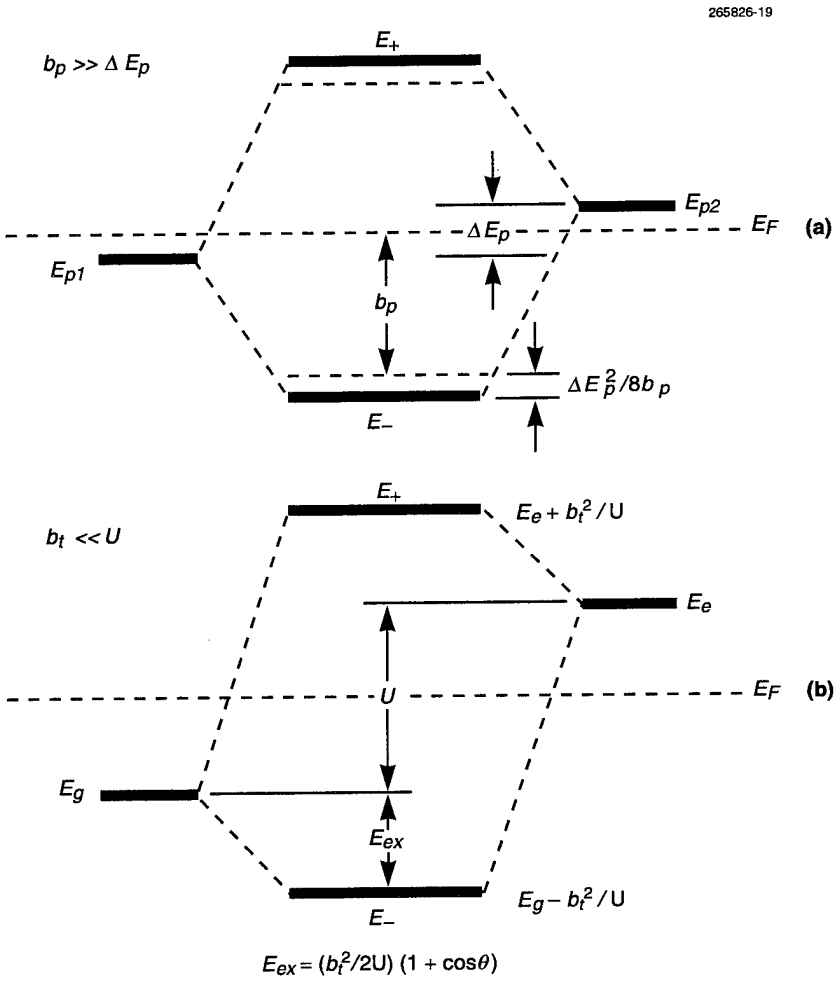

Figure A-1. Simple perturbation models for (a) charge transport between similar ions in sites of energy different by ΔE_p, and (b) charge transfer between similar ions in equivalent sites through an excited state of energy U.

where the Fermi energy $E_F = (E_{p2} + E_{p1})/2$, $\Delta E_p = E_{p2} - E_{p1}$, and $b_p = (E_{p2} + E_{p1})S$, where S is the overlap integral of the cation wave functions in the two polaron sites. For the $b_p >> \Delta E_p$ case of Figure A-1(a), the respective bonding (–) and antibonding (+) energies are

$$E_{\pm} = E_F \pm \left(b_p + \frac{\Delta E_p{}^2}{8 b_p} \right) \quad , \tag{A-3}$$

and the increase in bonding state energy due to the electrostatic potential energy ΔE_p is the basic or zero-spin activation energy for transport,

$$E_{hop}^0 = \frac{\Delta E_p{}^2}{8 b_p} \quad . \tag{A-4}$$

Magnetic Exchange Stabilization Energy. When an atom is ionized in free space, the removal (or addition) of an electron is accomplished at the cost of an ionization energy of many electron volts. In a crystal lattice this energy (e.g., the electronic work function) is reduced to a few electron volts because of the lower electrostatic fields due to polarizability of the dielectric medium. In cases where covalent bonding is significant, however, a less energy-expensive dynamic excitation takes place by charge transfer between cations through the covalent interaction with intermediate oxygen anions. Where selection rules are satisfied, the transfer can take place spontaneously.

Consider the case of Mn^{3+}-O^{2-}-Mn^{3+} where single electrons that occupy e_g orbitals of the two equivalent cations are covalently coupled through an O^{2-} ion. Because unpaired spins are present in the ground state manifold, a further limitation must be considered. This part involves the stabilization energy of the mobile carrier arising from magnetic exchange. According to Anderson's theory [4] of localized states, unpaired spins occupying similar orbitals of neighboring cations linked covalently by O^{2-} ions can lower the electronic system energy by energy-conserved exchanges of cation *d* electrons with 2*p* electrons of the oxygen anions. As sketched in Figure A-2, which is based on a version suggested by Pratt [26],[4] an excited state of energy U is created when two 2*p* electrons from the O^{2-} ions move to fill the half empty *d* states. Since the oxygen levels are now empty, the system can be restored to the ground state either by transferring the original cation *d* electrons to the O^{2-} ion or by recalling the 2*p* electrons. In the case of interest where an actual net charge transfer occurs between sites of equivalent energy (i.e., $\Delta E_p = 0$), the excited state may then be described by Figure A-2(b), with an oxygen 2*p* electron moving

---

[4] The original Anderson version of the excited state was created by the virtual transfer of one *d* electron from the first cation to the second cation, i.e.,

$$M_1{}^{n+} + M_2{}^{n+} \rightarrow M_1{}^{(n-1)+} + M_2{}^{(n+1)+} + U \quad ,$$

with the "exchange" completed by a return trip of the same electron. Although this concept ignored any role played by the intermediary O^{2-} ion, it produced a rationale for U, which was estimated as the difference in free cation ionization potentials (but without including the attendant increases in the lattice Madelung energy).

to the Mn^{4+} ion to set up a peroxide Mn^{3+}-O^{1-}-Mn^{3+} manifold. The eventual ground state then becomes dynamic, as the single *d* electron is shared between the two Mn^{4+} ions (and with any others on equivalent sites). The definition of U therefore is the energy required to effect the transfer where $b_t = 0$. It should be noted that the case of Figure A-2(a) produces antiferromagnetism, while that of Figure A-2(b) gives ferromagnetism.

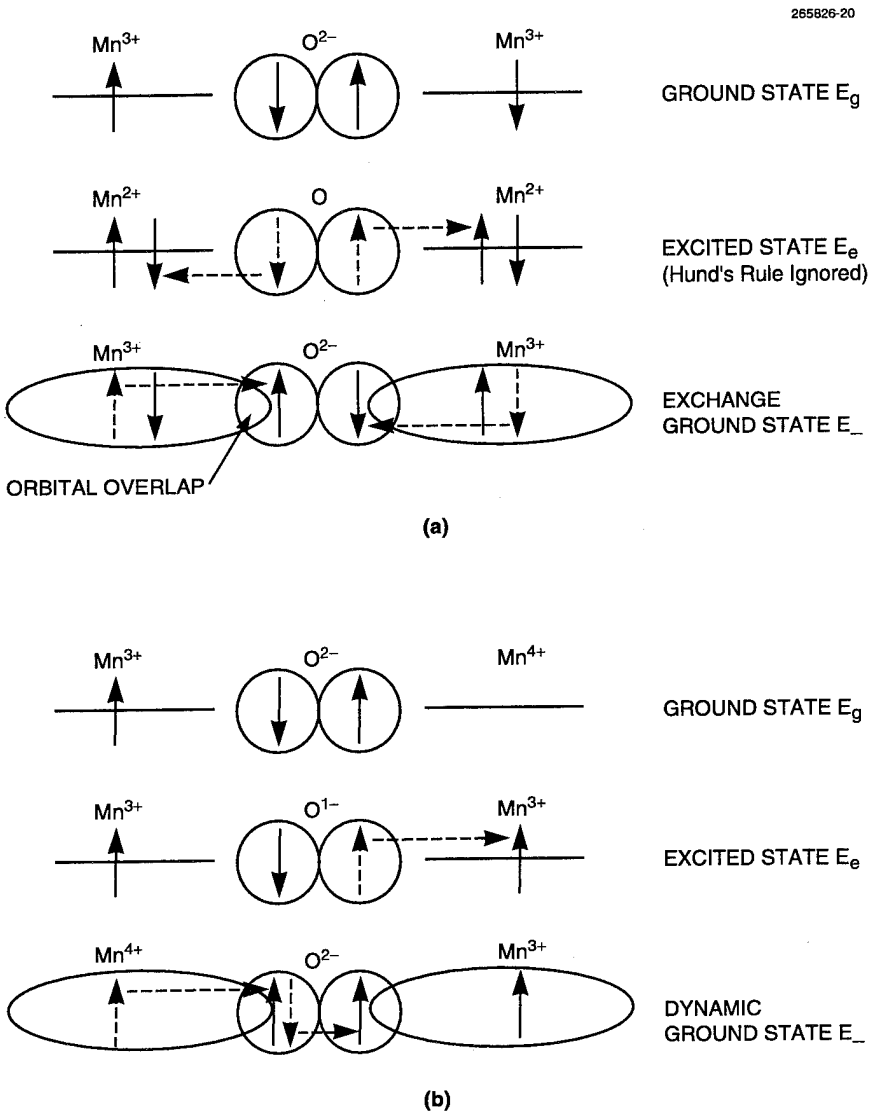

Figure A-2. Excited state models of electron transfer between neighboring cations involving the oxygen mediating oxygen ion for (a) two half-filled cation orbitals and (b) one half-filled and one empty cation orbital in which the lowest energy state is one that is stabilized by a kinetic transferring of electrons made possible by the overlapping of Mn 3d orbitals and O 2p orbitals.

For the transfer of electrons between equivalent sites[5] through a virtual excited state of energy U [e.g., Figure A-2(b)] and a transfer integral between cation and anion b_t depicted in Figure A-1(b), the secular equation is

$$\begin{vmatrix} \mathcal{H}_{11} - E & \mathcal{H}_{12} \\ \mathcal{H}_{12} & \mathcal{H}_{22} - E \end{vmatrix} = \begin{vmatrix} E_g - E & b_t \\ b_t & E_e - E \end{vmatrix} = 0 \quad . \tag{A-5}$$

The straightforward solution of the resulting quadratic equation is

$$E_{\pm} = E_{\mathrm{F}} \pm \frac{\sqrt{U^2 + 4{b_t}^2}}{2} \quad , \tag{A-6}$$

where the Fermi energy $E_{\mathrm{F}} = (E_e + E_g)/2$, $U = E_e - E_g$, and $b_t = (E_e + E_g)S$. For the case of $b_t << U$ of Figure A-1(b), the respective bonding (–) and antibonding (+) states are

$$E_{\pm} = E_{\mathrm{F}} \pm \left(\frac{U}{2} + \frac{{b_t}^2}{U} \right) \quad . \tag{A-7}$$

and the increase in bonding state energy due to charge transfer is

$$E_{ex} = \frac{{b_t}^2}{U} \quad . \tag{A-8}$$

For the case of transfer ions with unpaired spins, Anderson [4] reasoned that the transfer energy should be modified to account for the particular conditions of spin alignment required by the Pauli principle (Hund's rule) that is responsible for the $\Delta S = 0$ selection rule. With a canting angle θ_{ij} between spins i and j, the transfer integral is expressed as $b_t \cos(\theta_{ij}/2)$ and $b_t \sin(\theta_{ij}/2)$ for ferromagnetism and antiferromagnetism, respectively. In the ferromagnetic case of Figure A-1(b), the increase in binding energy due to the energy of the ion at site i gained from the transferring of charge among the ions at sites j may be defined from Equation (A-8) as

$$E_{ex} = \sum_j \frac{{b_t}^2}{U} \cos^2\left(\frac{\theta_{ij}}{2} \right) = \sum_j \frac{{b_t}^2}{2U} \left(1 + \cos\theta_{ij} \right) \quad . \tag{A-9}$$

The spin alignment contribution may be expressed in terms of Anderson's superexchange relation [4]:

---

[5] It should be pointed out that if the oxygen-involved excited state is also ignored in the mixed-valence case of real charge transfer, one is led to conclude that there is no excited state, i.e., $U = 0$. Consequently, first-order perturbation theory would apply, and the de Gennes explanation [10] of Zener's "double exchange" mechanism [9] would logically follow. If $U = 0$, however, the angular dependence of the exchange energy varies as $\cos(\theta_{ij}/2)$ instead of $\cos^2(\theta_{ij}/2)$ as in Equation (A-9). It may be shown that such a result allows the use of the conventional exchange Hamiltonian of Equation (1) only where $\cos\theta_{ij} << 1$, i.e., near $T = T_C$.

$$E_{ex}(\theta) = 2\sum_j J_{ij} S_i \cdot S_j \approx \sum_j \frac{b_t^2}{2U} \cos\theta_{ij} \quad , \tag{A-10}$$

where the smaller Hartree-Fock direct exchange contribution is ignored.

For an individual charge transfer between Mn^{3+} and Mn^{4+} ions depicted in Figure A-2(b), the E_{34} term may be extracted from Equation (A-10) with b_{34} and U_{34} referring to the b_t and $U$of the σ-bonded e_g and $2p$ orbitals of the respective Mn and O ions:

$$E_{34}(\theta) = 2zJ_{34} S_3 \cdot S_4 \approx z\frac{b_{34}^2}{2U_{34}} \cos\theta_{34} \quad , \tag{A-11}$$

where z is the number of nearest neighbors and θ_{34} is the average angle between the Mn^{3+} and Mn^{4+} spins, which will be assumed to be simply θ, the average angle between adjacent spins within the entire system. In this case, the factor of 2 that would reduce E_{34} because only one electron is involved has been absorbed into J_{34}. When $\theta = 0$, E_{34} has a maximum value of $2zJ_{34}S_3S_4$ and the spins are collinear to satisfy the $\Delta S = 0$ requirement for the charge transfer. If $\theta > 0$, E_{34} decreases, and energy must be provided to restore the spin alignment and maintain $\Delta S = 0$. Therefore, the additional energy has the effect of a magnetic trap of depth

$$E_{\text{hop}}{}^{ex} = E_{34}(\theta) - E_{34}(0) = 2zJ_{34}S_3S_4(1-\cos\theta) \quad , \tag{A-12}$$

and $E_{\text{hop}}{}^{ex}$ is also the activation energy necessary to effect the charge transfer between the two cation sites. It should be noted that θ values in the range 0 to π are allowed by Equation (A-12), and that the theoretical maximum activation energy from exchange is actually $2E_{\text{hop}}{}^{ex}$ when the spins are antiferromagnetic. For the current problem, however, the regime of interest is the ferromagnetic-to-paramagnetic transition that occurs at the Curie temperature, where the average angle between spins becomes π/2.

If the individual activation energies influence separate Boltzmann function carrier mobility probabilities p_p and p_{ex} for transport and transfer, respectively, a combined probability may be expressed as

$$p = p_p \cdot p_{ex} = \exp\left(\frac{-E_{\text{hop}}{}^0}{kT}\right) \cdot \exp\left(\frac{-E_{\text{hop}}{}^{ex}}{kT}\right) \tag{A-13}$$

and

$$E_{\text{hop}} = E_{\text{hop}}{}^0 + E_{\text{hop}}{}^{ex} = \frac{\Delta E_p^2}{8b_p} + z\frac{b_t^2}{2U}(1-\cos\theta) \quad . \tag{A-14}$$

To help appreciate the significance of Equation (A-14) from a quantitative standpoint, a comment on the magnitudes of the polaron trap, excited-state, and exchange energies is in order. Based on the approximation that the polaron electronic trap energy equals the Coulomb energy e^2/Ka, where $K = 25$ and $a = 4$ Å, $\Delta E_p \sim 0.15$ eV, while $U \sim 10$ eV from Anderson's assessment. If the charge transfer integral

b_t ~ 0.5 eV, as concluded in earlier work on the cuprates [15], the two activation energies are estimated as $E_{hop}{}^0$ ~0.005 eV, in agreement with the range of values determined from high-T_c superconductivity data of the cuprates [17], and $E_{hop}{}^{ex}$ ~ 0.1 eV for $z = 6$, in agreement with the value derived in this report from the interpretation of magnetoresistance data of the manganites.

Polarons and Hopping Electrons. The relative contributions to electrical conduction by covalent transfer (polarons) and thermal activation (hopping electrons) deserves further comment. As described in detail previously, in situations where the magnetic excange trap is negligible ($E_{hop}{}^{ex}$ ~ 0) because of ferromagnetic spin ordering or antiferromagnetic frustration due to $S = 0$ transfer ions, large polarons can exist to temperatures approaching that of Debye Θ_D [7].

If the temperature dependence of b_p is ignored (a reasonable assumption at very low temperatures), another estimate of the hopping electron threshold may be derived from Equation (A-2). Since the quantum mechanical probability for carrier occupancy of site 2 is $C_2{}^2$, a covalent transfer efficiency may be expressed as (based on the more complete molecular-orbital analysis in Dionne [15], Appendix B)

$$\eta = 2C_2{}^2 = 1 - \frac{\Delta E_p}{2b_p} \tag{A-15}$$

for $b_p >> \Delta E_p$. The factor of 2 multiplies $C_2{}^2$ to normalize the transport probability at 1.0 when $C_2{}^2 = 0.5$, where the carrier would be equally likely to occupy either site. If η is now equated to $p_p = \exp(-E_{hop}{}^0/kT)$, an upper threshold for the transition to hopping electron dominance may be estimated with the help of Equation (A-4):

$$T_{hop} = \left(\frac{1}{k}\right)\frac{E_{hop}}{ln\left(1 - \frac{\Delta E_p}{2b_p}\right)} \approx \left(\frac{1}{k}\right)\frac{\Delta E_p}{4} \tag{A-16}$$

It should be noted that Equation (A-16) is independent of b_p, which can only be true in the limit of $b_p >> \Delta E_p$ T_{hop} would be about 400 K, which suggests that when the reduction in b_p occurs through lengthening of the polaron lifetime by increased phonon interaction, the actual value of T_{hop} is likely to be much lower.

Below the Curie temperature, the partitioning of coherent and incoherent conductivity is not an important factor in the magnetoresistance effects of the manganites. The statistical distribution of polarons and hopping electrons has little bearing on the metallic resistivity region, since the activated carriers also have a positive slope behavior above the $kT = E_{hop}{}^0$ threshold. For the high-T_c cuprates, however, the fraction of coherent carriers is crucial in determining the potential supercarrier density, which in turn sets the value of the critical temperature and a variety of other important superconductor parameters [15–17, 27].

REPORT DOCUMENTATION PAGE

Form Approved
OMB No. 0704-0188

1. AGENCY USE ONLY (*Leave blank*)	2. REPORT DATE	3. REPORT TYPE AND DATES COVERED
	20 May 1996	Technical Report

4. TITLE AND SUBTITLE

Anomalous Magnetoresistance in the Lanthanide Manganates and Its Relation to High-T_c Superconductivity

5. FUNDING NUMBERS

C — F19628-95-C-0002
PR — 1

6. AUTHOR(S)

Gerald F. Dionne

7. PERFORMING ORGANIZATION NAME(S) AND ADDRESS(ES)

Lincoln Laboratory, MIT
244 Wood Street
Lexington, MA 02173-9108

8. PERFORMING ORGANIZATION REPORT NUMBER

TR-1029

9. SPONSORING/MONITORING AGENCY NAME(S) AND ADDRESS(ES)

U.S. Air Force ESC
Hanscom AFB
Bedford, MA 01730

10. SPONSORING/MONITORING AGENCY REPORT NUMBER

ESC-TR-95-058

11. SUPPLEMENTARY NOTES

None

12a. DISTRIBUTION/AVAILABILITY STATEMENT

Approved for public release; distribution is unlimited.

12b. DISTRIBUTION CODE

13. ABSTRACT (*Maximum 200 words*)

A theory of electron transport is formulated from the polaronic and magnetic exchange character of mixed-valence transition metal oxides. Where magnetic ordering is established at low temperatures, the conduction is mainly by polarons. Above the curve temperature T_C, electron hopping by thermal activation becomes dominant. The conventional relations for mobility-activated semiconduction and the molecular field theory of ferromagnetism are adapted for interpretation of electrical resisivity ρ data of the lanthanide (rare-earth—*RE*) manganites $(RE^{3+}{}_{1-x}A^{2+}{}_{x})\,MnO_3$ as functions of temperature and external magnetic field. Computed results are consistent with the original resistivity data and agree quantitatively with the more recently observed magnetoresistance in film versions of this oxide system. The anomalies in electrical behavior are related to the superexchange couplings derived from σ and π bonding of the various 3*d* orbital states among $Mn^{2+}(3d^5)$, $Mn^{3+}(3d^4)$, and $Mn^{4+}(3d^3)$ ions in 180° metal-oxygen-metal configurations. The resistivity maximum occurs at the susceptibility peak slightly above T_C, and its magnitude is determined principally by the factor $[(1-x)/x]\,(kT_C)\exp(E_{hop}/kT_C)$, where the activation energy E_{hop} is the sum of a polaron trap energy $E_{hop}{}^{0}$(~ 5 meV) and a spin polarization-dependent component $E_{hop}{}^{ex}[1-B_S(T,H)]$, and B_S is the Brillouin function. For $T \geq T_C$, ferromagnetic spin alignment becomes disordered and E_{hop} increases to a value ~ 0.1 eV equal to the decrease in stabilization energy of the transfer electrons caused by the transition from spin alignment to disorder, i.e., $B_S = 0$. If E_{hop} is independent of temperature above T_C, the maximum sensitivity $d\rho/dH$, which occurs at $T = T_C$, may be exclusively a function of T_C through the function $(1/kT_C)\exp(E_{hop}/kT_C)$. The relative sensitivity $(1/\rho)\,d\rho/dH$, however, is not dependent on the exponential factor but is proportionally to $1/T_C{}^2$. As expected, the magnetoresistance sensitivities favor uniformity of T_C, and consequently a high degree of chemical homogeneity in the material

A similarity exists between the metallic ρ of the multivalent maganites at low temperatures and that of superconducting cuprates. In both cases the basic theory of the hopping electron semiconductor applies with almost identical values of lattice parameter and Debye frequency. However, the magnetic exchange contributions to E_{hop} in the manganite system differs from that of the cuprates. In the former case, the sharp decrease in the ferromagnetic exchange field at T_C enhances the magnetic field influence on ρ. It also correspondingly raises E_{hop} to reverse the resistivity from metallic to insulating. In the latter case, the absence of long range antiferromagnetic order due to the presence of zero-spin Cu^{3+} ions removes the exchange contribution to E_{hop}. In both the manganites and cuprates, it is concluded that metallic resistivity occurs because of the absence of an exchange trap.

14. SUBJECT TERMS

colossal magnetoresistance, high-T_c superconductivity, Curie temperatures, Brillouin functions, large polarons, Mn perovskites, hopping electrons, Jahn-Teller effects, Cu perovskites

15. NUMBER OF PAGES
52

16. PRICE CODE

17. SECURITY CLASSIFICATION OF REPORT	18. SECURITY CLASSIFICATION OF THIS PAGE	19. SECURITY CLASSIFICATION OF ABSTRACT	20. LIMITATION OF ABSTRACT
Unclassified	Unclassified	Unclassified	Same as Report